A STUDY ON THE ADSORPTION PROPERTIES OF QUATERNIZED CELLULOSE

Except where reference is made to the work of others, the work described in this dissertation is my own or was done in collaboration with my advisory committee. This dissertation does not include proprietary or classified information.

_____

Weijun Wang

Certificate of Approval:

_____	_____
Aliecia R. McClain, Co-Chair Assistant Professor Textile Engineering	Roy M. Broughton, Co-Chair Professor Textile Engineering
_____	_____
Peter Schwartz Professor Textile Engineering	Ann Beth Jenkins Presley Associate Professor Consumer Affairs

_____

Stephen L. McFarland
Dean
Graduate School

A STUDY ON THE ADSORPTION PROPERTIES OF QUATERNIZED CELLULOSE

Weijun Wang

A Dissertation

Submitted to

the Graduate Faculty of

Auburn University

in Partial Fulfillment of the

Requirements for the

Degree of

Doctor of Philosophy

Auburn, Alabama
December 16, 2005

A STUDY ON THE ADSORPTION PROPERTIES OF QUATERNIZED CELLULOSE

Weijun Wang

Permission is granted to Auburn University to make copies of this thesis at its discretion, upon the request of individuals or institutions and at their expense. The author reserves all publication rights.

_____

Signature of Author

_____

Date of Signature

VITA

Weijun Wang, son of Panying Wang and Tianshen Zhou, was born on July 28, 1962, in Shanghai, People's Republic of China. He was graduated from China Textile University in Textile Chemistry Engineering Department in 1982. After working as a textile research engineer in China Textile University's Man-made Fiber Research Institute, he was invited to Textile Engineering Department in Auburn University as a visiting scholar in 1997. He entered the masters program in Integrated Textile and Apparel Science at Auburn University in June 2000 and received the degree of Master of Science in December 2002. He married Yiping Lu, daughter of Linhu Lu and Fengxiang Wang, on April 28, 1992. They have a son, Di Wang.

DISSERTATION ABSTRACT

A STUDY ON THE ADSORPTION PROPERTIES OF QUATERNIZED CELLULOSE

Weijun Wang

Doctor of Philosophy, December 16, 2005
(M. S., Auburn University, 2002)
(Diploma, China Textile University, 1982)

110 Typed Pages

Directed by Roy M. Broughton and Aliecia R. McClain

The dissertation consists of four chapters: Literature Review, Anionic Dye Decolorization from Textile Wastewater, the Characterization of the Surface Thermodynamics of Quaternized Cellulose Fiber by Inverse Gas Chromatography, and Study on the Correlations between the Surface Characteristics and Adsorption Capabilities of Quaternized Cellulose Fiber.

In the first chapter, the resources of cellulose, chemical and physical properties of cellulose, and functionlization methods of cellulose are reviewed. Recent studies are summarized as well.

In the second chapter, an efficient way to remove the anionic dye for textile

wastewater is presented. The results of the treatment of cellulose (recycled newsprint) with 3-Chloro-2-Hydroxy-N,N,N-Trimethyl-1-Propanaminium Chloride (quaternary ammonium) indicate that the nitrogen contents depend greatly on the pH. The optimum pH is higher than 10 and less than 13. Increasing the amount of quaternary ammonium on cellulose fiber increases the number of dye bonding sites and breaks up more hydrogen bonds at the same time. Decreasing hydrogen bonding results in more swollen macrostructures, which increases time to access to the dye bonding sites. Therefore the dye removal kinetic is not only depended on the concentration of attached quaternary ammonium groups but also on the surface of fibers. It is also controlled by the number of dye sites inside the wall of the pores or the channels. The process of dye removal for quaternized cellulose can be completed within seconds when the concentration of dye less than 220 mg/l at room temperature. The saturation value of quaternized cellulose is 10 times higher than that of activated carbon and the quaternized cellulose exhibits an extremely high capability for dye adsorption.

In the third chapter, the surface thermodynamics of quaternized cellulose fibers are characterized by inverse gas chromatography (IGC) using specific gas probes over different temperature. Surface energy characteristics (such as interaction enthalpy, the dispersive component of the surface energy), and acid-base properties of the quaternized cellulose surface have been quantified.

The data generated in this study is derived from the fundamental parameter in IGC measurements, the specific retention volume by injecting neutral probes such as saturated n-alkanes and by injecting amphoteric, acidic and basic probes such as acetone,

chloroform and THF. The dispersive components of surface energy derived from the net retention values of n-alkanes are correlated with the supermolecular structures of cellulose. According to X-ray and FT-IR data, the dispersive components of surface energy decrease with increasing the crystallinity. The data obtained from IGC experiments by injecting amphoteric, acidic and basic probes show that the surface of the cellulose becomes more basic than acidic after quaternization in terms of electron acceptor and electron donor constants, that is as indicated by the Lewis acidity and Lewis basicity constants, K_A and K_D. The FT-IR results indicate that the changes of surface properties result from changes of chemical constitution after quaternization. It is proposed that the driving force for surface adsorption is the heat of the Lewis acid-base interaction between quaternized cellulose and anionic dyes.

In the fourth chapter, the surface characteristics of the cellulose fiber are shown to play a very important role in the adsorption capacity. The correlation between the surface characteristics and adsorption capability of quaternized cellulose is established. The study shows that the fine structure of cellulose fibers does not affect their adsorption capability of cellulose, and the adsorption capability of cellulose is dramatically increased after qauterniztion. The mechanical treatment, beating, improves the surface properties preferable for qauternization and adsorption. The mechanism for increasing adsorption capability is that an electron donor group, an ether functional group, and a cationic functional group are introduced onto the polymer backbone of cellulose by quaternization. Therefore the acid-base interactions and ionic bonding could strongly affect the adsorption capability. This study might supply useful information for selecting

the best adsorbates and adsorbents in terms of K_A and K_B, the electron donor and accepter constants.

ACKNOWLEDGMENTS

The author would like to express his utmost gratitude to his advisors, Dr. Roy M. Broughton and Dr. Aliecia R. McClain, for always providing the patient guidance and atmosphere of respect that made this work possible. The author also expresses his gratitude to the other members of his advisory committee, Dr. Peter Schwarz, Dr. Ann Beth Jenkins Presley, and outside reader, Dr. Mills for their interest, understanding and timely invaluable advice.

The author's appreciation from the bottom of his heart also goes to Dr. David M. Hall for his generous chemical supplies and his valuable advices and to the head of the Department of Textile Engineering, Dr. Schwartz, as well as the Department of Textile Engineering for their financial supports.

Thanks are also due to his wife, Yiping Lu, and his son, Di Wang, for their unwavering love and encouragement.

Style manual or journal used THE ACS STYLE GUIDE: A MANUAL FOR AUTHORS AND EDITORS

Computer software used MICROSOFT WORD 2000

TABLE OF CONTENTS

DISSERTATION ABSTRACT v

LIST OF FIGURES xvii

LIST OF TABLES xx

CHAPTER 1 LITERATURE REVIEW 1

1.1 Introduction 1

1.2 Sources of Cellulose 1

1.3 Chemical Structure and Composition of Cellulose 2

1.4 The Supermolecular Structures of cellulose 2

1.5 Hydrogen Bonding 6

1.6 Reactions of Cellulose 7

1.6.1 General Consideration 7

1.6.2 Esterification 8

1.6.2.1 Organic Esters 9

1.6.2.2 Inorganic Esters 10

1.6.3 New Cellulose Esters 11

1.7 Etherification 12

1.7.1 Carboxymethylcellulose 13

1.7.2 Hydroxyethylcellulose and hydroxypropycellulose 14
1.7.3 Alkyl ethers of cellulose 15
1.8 Grafting 16
1.9 Deoxyhalogenation 18
1.10 Oxidation 19
1.11 A example of Anionic Ion Exchanger from Cellulose 20
1.12 Two examples of Cationic Ion Exchanger from Cellulose 21
1.13 The research efforts of quaternized cellulose for color removal during a decade 23
1.14 Summery 24
1.15 References 25

CHAPTER 2 ANIONIC DYE DECOLORIZATION FROM TEXTILE WASTE WATER 29
2.1 Introduction 29
2.2 Experimental 30
2.2.1 Materials 30
2.2.2 Pretreatment of Recycled Newsprint (Mercerization) 30
2.2.3 Pretreatment of Recycled Newsprint (Water Swelled) 31
2.2.4 Cellulose Quaternization Reaction (Cationization) 31
2.2.5 Cationization: Method A 32

2.2.6 Cationization: Method B 33

2.2.7 Effect of Quat Concentrations on Nitrogen Contents 33

2.2.8 Effect of pH conditions on Nitrogen Contents 33

2.2.9 NNitrogen Analysis 34

2.2.10 Water Retention and Moisture Regain Tests 34

2.2.11 Precipitation Observation 34

2.2.12 Removal Dye Kinetics 34

2.2.13 Dye Adsorption Isotherm 35

2.3 Results and Discussion 36

2.3.1 Nitrogen Analysis 36

2.3.2 Effects of Quat Concentrations and pH conditions on Nitrogen Contents 36

2.3.3 Water Retention and Moisture Regain 38

2.3.4 Precipitation Speed 40

2.3.5 The Removal Dye Kinetics 40

2.3.6 Dyeing Adsorption Isotherm 42

2.3.7 Relationship between Saturate Value and Nitrogen Contents 48

2.4 Conclusions 49

2.5 References 51

CHAPTER 3 THE CHARACTERIZATION OF THE SURFACE THERMODYNAMICS OF QUATERNIZED CELLULOSE FIBER BY INVERSE GAS CHROMATOGRAPHY 52

3.1 Introduction 52

3.2 Experimental 58

3.2.1 Materials 58

3.2.2 Methods 59

3.2.2.1 Fiber Treatments 59

3.2.2.2 Inverse Gas Chromatography 59

3.2.2.3 Moisture Regains 60

3.2.2.4 Crystallinity 60

3.2.2.5 Analysis of Chemical Constitution 61

3.2.2.6 Scanning Electron Microscopy (SEM) 61

3.3 Results and Discussions 61

3.4 Conclusions 72

3.5 References 73

CHAPTER 4 STUDY ON THE CORRELATIONS BETWEEN THE SURFACE CHARACTERISTICS AND ADSORPTION CAPABILITY OF QUATERNIZED CELLULOSE FIBER 75

4.1 Introduction 75

4.2 Experimental 77

4.2.1 Materials 77

4.2.2 Methods 77

4.2.2.1 Fiber Treatments 77

4.2.2.2 Measurements of Freeness 77

4.2.2.3 Qauternization of Beaten Fibers 77

4.2.2.4 Nitrogen Analysis 78

4.2.2.5 Chemical Constitute Analysis 78

4.2.2.6 Scanning Electron Microscopy (SEM) 78

4.2.2.7 Kinetic Dye Adsorption 78

4.2.2.8 Adsorption Isotherm 78

4.3 Results and Dissuasions 79

4.3.1 Fine Structures verse Base-Acid Interaction on Dye Adsorption 79

4.3.2 Surface Areas verse Base-Acid Interaction on Dye Adsorption 81

4.4 Conclusions 90

4.5 References 91

LIST OF FIGURES

Figure 1-1 Molecular structure of cellulose including numbering of C-atoms 3

Figure 1-2 Fine structure of cellulose fiber 4

Figure 1-3 Interconversion of the polymorphs of cellulose 4

Figure 1-4 Unit cell structure of native cellulose I and of mercerized cellulose II 6

Figure 1-5 Intramolecular hydrogen bonding 7

Figure 1-6 Intermolecular hydrogen bonding 7

Figure 1-7 Positions in cellulose structure for chemical modifications 8

Figure 1-8 Chemical structures of fluorine-containing cellulose esters 12

Figure 1-9 Chemical structures of new cellulose ethers 15

Figure 1-10 Cellulose fiber before grafting 17

Figure 1-11 Cellulose fiber after grafting 17

Figure 1-12 Deoxyhalogenation of cellulose 18

Figure 1-13 Oxidation of cellulose 19

Figure 1-14 A schematic depicting the special relationships of the functional groups grafted onto the polysaccharide backbone 23

Figure 2-1 Conversion of the quat chlorohydrin to the epoxy form 31

Figure 2-2 Reaction of the quat epoxy with cellulose fiber 32

Figure 2-3 The effect of quat concentrations on the nitrogen contents on the quat cellulose fibers 37

Figure 2-4 The effect of pH on the nitrogen contents at 10% quat 38

Figure 2-5 The relationship between moisture regain and the nitrogen contents on the quat cellulose fibers 39

Figure 2-6 The relationship between water retention and the nitrogen contents on the quat cellulose fibers 39

Figure 2-7 The precipitation rate after 24 hour settling time 40

Figure 2-8 The concentration of dye remaining in solution vs. time 42

Figure 2-9 Adsorption isotherm of sample S3 44

Figure 2-10 Adsorption isotherm of sample S3 44

Figure 2-11 Adsorption isotherm of sample S1 46

Figure 2-12 Adsorption Isotherm of Sample S1 46

Figure 2-13 The saturation values verse nitrogen contents 49

Figure 3-1 Variation of the logarithm of the net retention volume of n-alkanes versus 2N*a* $\sqrt{\gamma_L^D}$ of probes 55

Figure 3-2 Representation of IGC data used for the determination of ΔG^{sp} for the specific probes 56

Figure 3-3 Representation of IGC data used for the determination of ΔH^{sp} for specific probes 57

Figure 3-4 Plot of $\Delta H^{sp}/AN$ as a function of DN/AN allowing the determination of the acceptor constant K_A and the donor constant K_D 57

Figure 3-5 The net retention time of n-alkanes at different temperature for Sample A (control sample) 62

Figure 3-6 The net retention time of n-alkanes at different temperature for Sample B (mercerized sample) 62

Figure 3-7 The net retention time of n-alkanes at different temperature for Sample D (quaternized sample) 63

Figure 3-8 The values of γ_S^D versus the temperature 64

Figure 3-9 Fine structure of cellulose fiber 65

Figure 3-10 FT-IR spectra for sample A, sample B, and sample D 67

Figure 3-11 Topological observation of sample A. (a) ×500, (b) ×2000 68

Figure 3-12 Topological observation of sample B. (a) ×500, (b) ×2000 69

Figure 3-13 Topological observation of sample D. (a) ×500, (b) ×2000 69

Figure 3-14 X-ray diffraction curves 70

Figure 4-1 Kinetic dye adsorption 80

Figure 4-2 The Morphology of Control Sample (a) ×500, (b) ×2000 83

Figure 4-3 The Morphology of Beaten Sample at 50 Min (a) ×500, (b) ×2000 83

Figure 4-4 The values of γ_S^D versus the temperature 84

Figure 4-5 FT-IR spectra for sample 0 and sample 50 84

Figure 4-6 Adsorption isotherm for samples 0 and 50 85

Figure 4-7 Adsorption isotherm for samples 0-N and 50-N 86

Figure 4-8 Adsorption Isotherm for samples 50-N and 50-N-30 86

Figure 4-9 Chemical bonds and interactions between an anionic dye and the quaternized cellulose 88

LIST OF TABLES

Table1-1 Chemical composition of some cellulose resources 2

Table 2-1 Nitrogen analysis results under different conditions 36

Table 2-2 Comparison of the parameters from fitting to Langmuir model with activated carbon 47

Table 2-3 The proportion of molar numbers of dye and qaut 48

Table 3-1 Characteristics of IGC probes used in experiment 58

Table 3-2 The X-ray crystallinity index (CrI), FT-IR total crystallinity index (TCI), moisture regain (MR), and accessibility of the samples 65

Table 3-3 The enthalpy and the entropy of adsorption of the specific probes 71

Table 3-4 Comparison of K_A and K_D 71

Table 4-1 The enthalpy and the entropy of adsorption of the specific probes 80

Table 4-2 Comparison of K_A and K_D 81

Table 4-3 Comparison of saturation values 81

Table 4-4 The freeness and nitrogen contents of beaten samples 82

Table 4-5 The saturation values for different nitrogen contents 87

Table 4-6 The enthalpy and the entropy of adsorption of the specific probes 89

Table 4-7 Comparison of the dye affinity and saturation values of quaternized cellulose with different beating time reaction time samples 89

Table 4-8. The proportion of molar numbers of dye and quat 89

CHAPTER 1

LITERATURE REVIEW

1.1 Introduction

Cellulosic materials are reasonable strong, hydrophilic, insoluble in water, insoluble in organic solvents, safe to living organisms, reproducible, recyclable, and biodegradable. Many technologies have been applied to produce modified cellulosic materials for our daily and industrial necessities.

Cellulosic materials are particularly attractive in this research because cellulose is the most abundant resource of naturally occurring polymers on the earth. The chemical structure and composition of cellulose determine its chemical and physical properties. Cellulose has been used as a substrate for chemical modifications even before its polymeric nature was recognized and well understood. In this review, the history of the modification of cellulose is summarized and divided into three periods according to the different market demands. The chemical modifications of cellulose involved esterification, etherification, grafting, deoxyhalogenation, and oxidation.

1. 2 Sources of Cellulose

Cellulose is the most abundant natural polymer in the world. There are three Types of Cellulosic Materials:

- Primary cellulosics: plant harvested for cellulose such as cotton, timber, hay, etc.
- Agricultural Waste Cellulosics: plant material remaining after harvesting such as straw, corn stalks, rice hulls, sugar cane etc.

- Municipal Waste Cellulosics: cellulose containing waste from cities such as waste paper, yard debris, etc.

Commercial cellulose production concentrates on easily harvested sources such as wood or on the highly pure sources such as cotton. Table 1-1 gives us the composition of different cellulose resources.

Table1-1. Chemical composition of some cellulose resources (Hon, 1996)

Source	Composition (%)			
	Cellulose	Hemicellulose	Lignin	Extract
Wheat straw	30	50	15	5
Bagasse	40	30	20	10
Softwood	4-44	25-29	25-31	1-5
Hardwood	43-47	25-35	16-24	2-8
Flax (retted)	71.2	20.6	2.2	6.0
Jute	71.5	13.6	13.1	1.8
Henequen	77.6	4.8	13.1	3.6
Ramie	76.2	16.7	0.7	6.4
Cotton	95	2	0.9	0.4

1.3 Chemical Structure and Composition of Cellulose

Whereas hemicellulose has an extremely heterogeneous chemical composition, cellulose is a chemically homogeneous linear polymer of up to 10,000 D-glucose molecules, which are connected by β-1,4 bonds (see Figure 1-1) (Heinze, 2001). Because each glucose residue is tilted by 180° towards its neighbor, the structural subunit of cellulose is cellobiose. The chemical uniformity allows spontaneous crystallization of the cellulose molecules. Hydrogen bonding within and between multiple layers of parallel molecules results in the formation of tightly packed microfibrils.

1.4 The Supermolecular Structures of cellulose

The cellulose fibers consist of elementary fibrils, which are a succession of

crystallites and intermediate less-ordered amorphous regions (Figure 1-2). The crystallites (A) are characterized by their size and their orientation. Less-ordered amorphous regions (B) connect successive crystallites length-wise; they are characterized by their size, density, and orientation. Lateral tie molecules-region (C) connects laterally adjacent amorphous regions. The cluster formations (D) are regions where crystallites are fused to large aggregates and region (E) represents the voids (Stana-Kleinschek et al., 2001). The amorphous regions and inner surface area of voids affect significantly the accessibility, reactivity and adsorption properties of fibers.

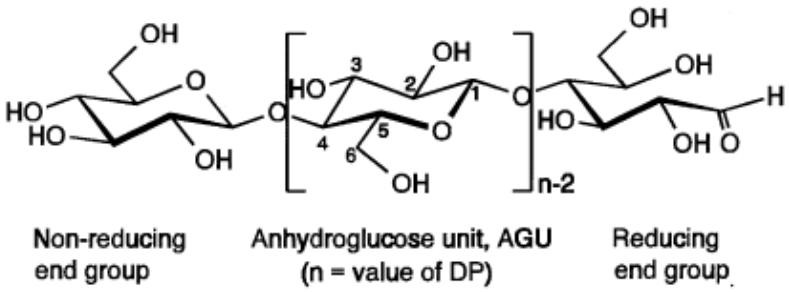

Figure 1-1. *Molecular structure of cellulose including numbering of C-atoms.*

There are two main accessibilities. One is that of the low-ordered regions which constitute the amorphous regions in the fringed micellar model, or the connecting chains and disordered parts of the elementary fibrils in the fibrillar model, extending across the fibrils periodically along their length. It would also include the lateral layers separating the adjacent elementary fibrils from each other; the surfaces between consecutive crystal blocks (see B, C, and E regions in Figure 1-2). The second accessibility is that of the surfaces of the crystallites (see A and D regions in Figure 1- 2).

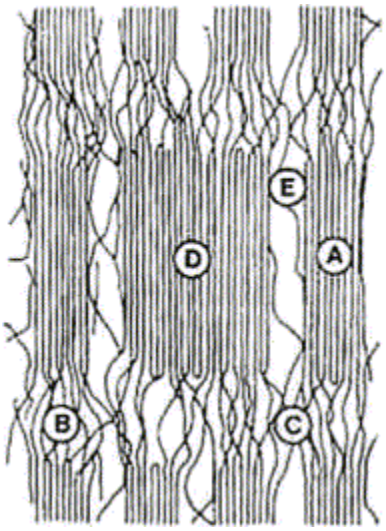

Figure 1-2. *Fine structure of cellulose fiber—schematically: A, crystallites; B, amorphous regions; C, interfibrillar tie molecules; D, cluster formation; E, void (Stana-Kleinschek et al., 2001).*

The polymorphism of cellulose and its derivatives has been well documented. Six polymorphs of cellulose (I, II, III_1, III_{11}, IV_1 and IV_{11}) can be interconverted, as shown in Figure 1-3 (Marchessault and Sarko, 1967; Hayashi et al., 1987; Marchessault and Sundararajan, 1983).

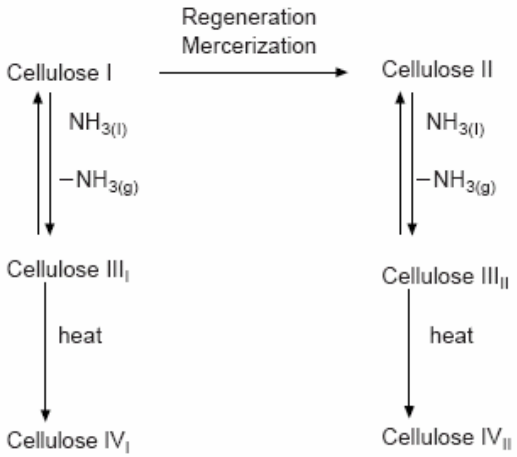

Figure 1-3. *Interconversion of the polymorphs of cellulose.*

More recently, evidence for two polymorphs of cellulose I has been offered (VanderHart and Atalla, 1984; Sugiyama et al., 1991); that is to say what was previously thought to be polymorph (I) has now been found to be a mixture of two polymorphs (I_α and I_β). Proof of the polymorphy of cellulose was obtained from nuclear magnetic resonance (NMR), infrared and diffraction studies (Blackwell and Marchessault, 1971; Blackwell, 1982). Cellulose I, or native cellulose, is the form found in nature. Cellulose II, the second most extensively studied form, may be obtained from cellulose I by either of two processes: a) regeneration, which is the solubilization of cellulose I in a solvent followed by reprecipitation by dilution in water to give cellulose II, or b) mercerization, which is the process of swelling native fibers in concentrated sodium hydroxide, to yield cellulose II on removal of the swelling agent. Celluloses III_1 and III_{11} (Marrinan and Mann, 1956; Hayashi et al., 1975) are formed, in a reversible process, from celluloses I and II, respectively, by treatment with liquid ammonia or some amines, and the subsequent evaporation of excess ammonia (Davis et al., 1943; Sarko et al., 1976). Polymorphs IV_1 and IV_{11} (Hess and Kissig, 1941 and Sarko, 1987) may be prepared by heating celluloses III_1 and III_{11} respectively, to 206 ^oC, in glycerol (Wada et al., 2004).

Although cellulose forms some distinct crystalline structures, cellulose fibers in nature are not purely crystalline, but with all degrees of order from crystalline to amorphous. Regardless of their orientation, the chains are stiffened by both intrachain and interchain hydrogen bonds. The crystalline nature of cellulose implies a structural order in which all of the atoms are fixed in discrete positions with respect to one another. An important feature of the crystalline array is that the component molecules of individual

microfibrils are packed sufficiently tightly to prevent penetration not only by dye molecules but even by small molecules such as water. In addition to the crystalline and amorphous regions, cellulose fibers contain various types of irregularities, such as kinks or twists of the microfibrils, or voids such as surface micropores, large pits, and capillaries. The total surface area of a cellulose fiber is, thus, much greater than the surface area of an ideally smooth fiber of the same dimension. The net effect of structural heterogeneity within the fiber is that the fibers are at least partially hydrated by water when immersed in aqueous media, and some microspores and capillaries are sufficiently spacious to permit penetration by relatively large molecules such as dyestuff molecules. The dimensions of Meyer-Mark-Misch and Andress crystal lattice are shown in Figure 1-4 (Kennedy et al., 1985).

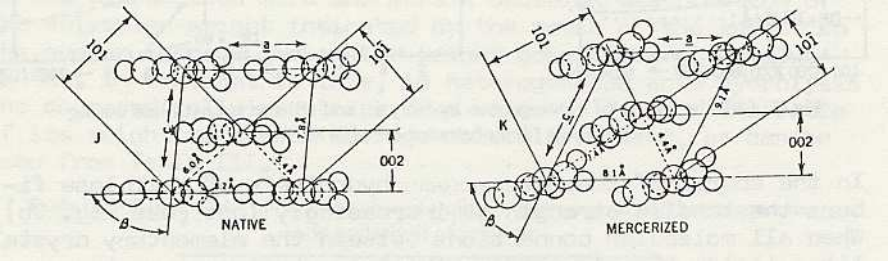

Figure 1-4. *Unit cell structure of native cellulose I (Meyer, Mark, and Misch) and of mercerized cellulose II (Andress).*

1.5 Hydrogen Bonding

Each glucose of cellulose has three hydroxyl groups. Therefore, hydrogen bonding plays a very important role in physical and chemical properties. The molecular motion of cellulose is restricted by inter- and intra-molecular hydrogen bonding. Each chain forms two intramolecular hydrogen bonds: O3'-H…O5' as proposed by Hermans

et al. from (Hermans et al., 1943) a study of spacing-filling models, and O2'-H…O6', as suggested by the polarized infrared spectra (Marrinan and Mann 1956; Jones, 1958) (see Figure 1-5). There is also an intermolecular hydrogen bond, O6'-H…O3'; linking adjacent chains in sheets (see Figure 1-6).

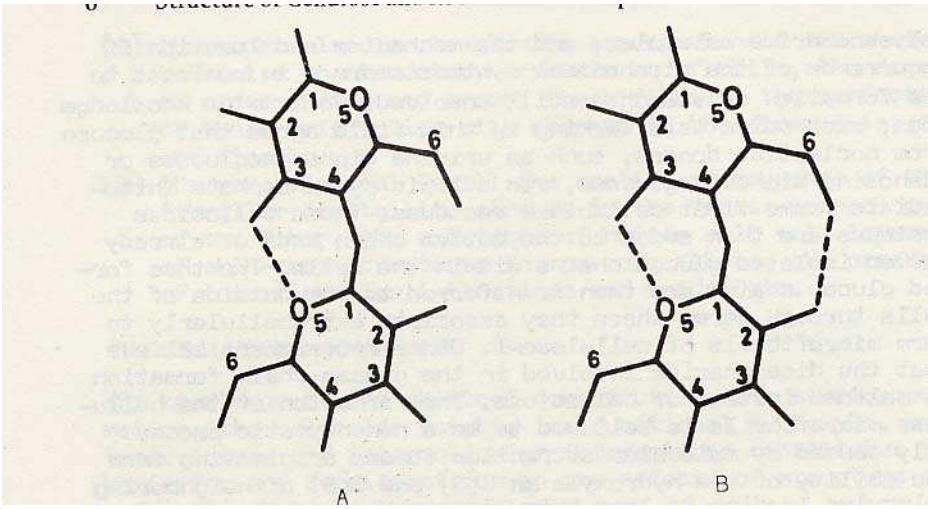

***Figure 1-5**. Intramolecular hydrogen bonding.*

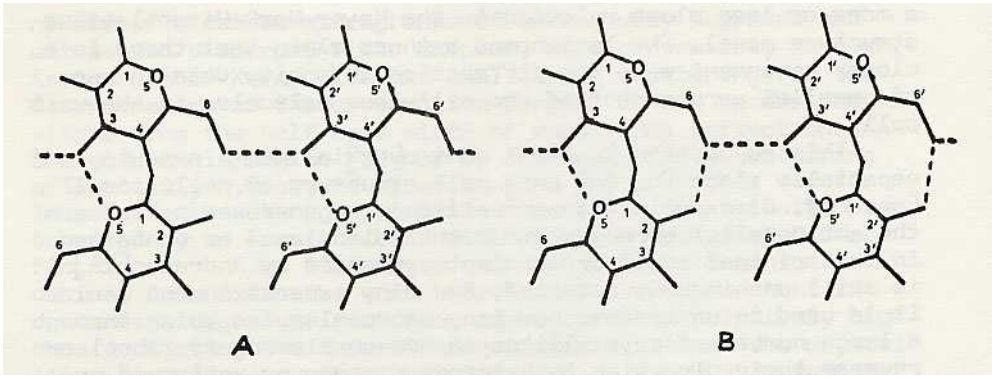

***Figure 1-6**. Intermolecular hydrogen bonding.*

1.6 Reactions of Cellulose

1.6.1 General Consideration

The typical modifications of cellulose are esterification and etherifications of

hydroxyl groups. Most soluble cellulose derivatives are prepared by these substitution reactions which allow drastic changes in the original properties of cellulose to be achieved. Others modifications include ionic and radical grafting, acetalation, deoxyhalogenation, and oxidation. Since the usual cellulosic materials originating from wood and cotton pulps have aldehyde and carboxyl groups in quite small quantities, depending on the purity of the pulps, these minor groups are also target positions for chemical modification. Figure 1-7 shows schematic representation of positions in the cellulose structure for chemical modifications.

The relative reactivity of the hydroxyl groups varies from one reaction to another. Usually the reaction varies in the order of OH-6 >> OH-2 > OH-3 (Nevell, 1985).

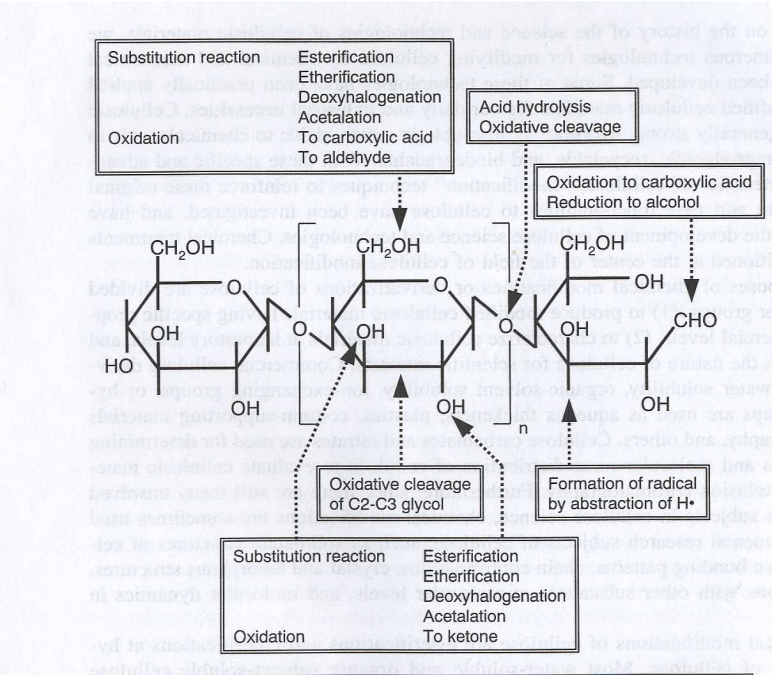

Figure 1-7. *Positions in cellulose structure for chemical modifications.*

1.6.2 Esterification

Since cellulose is an alcohol, it undergoes esterification with acids in the presence

of a dehydrating agent or by reaction with acid chlorides. The resulting esters have entirely different physical and chemical properties from the original cellulose and are soluble in a wide range of solvents. The cellulose esters are divided into organic esters and inorganic esters (Nevell and Zeronian, 1985) according the reactant.

1.6.2.1 Organic Esters

1. Cellulose acetate

Cellulose acetate is universally recognized as the most important organic ester of cellulose owing to its extensive applications in fibers, plastics, and coatings. Cellulose acetates are prepared by reacting high purity cellulose with acetic anhydride, utilizing acetic acid as the solvent and sulfuric acid as a catalyst (Tanghe et al., 1963). The secondary acetate and triacetate are obtained by following reactions:

Secondary acetate:

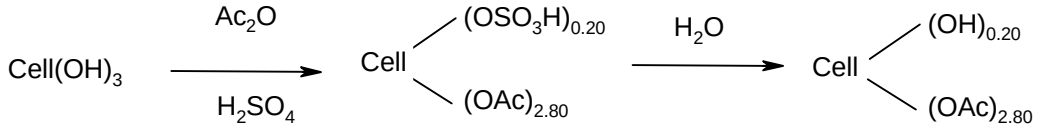

Triacetate:

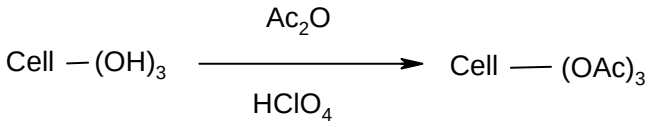

2. Esters of other aliphatic acids

Other esters such as cellulose formate, cellulose propionate and butyrate are prepared similarly to the acetates, but in much smaller quantities. Formic acid will esterify cellulose in the presence of a catalyst, producing mono-and di-formates. Catalysts typically used, such as H_2SO_4, HCl(g), $ZnCl_2$, or P_2O_5, are not needed when the

more reactive regenerated cellulose is the starting material (Novell, 1985).

3. Carbamate esters

Cellulose carbamates (urethanes) are prepared by the action of isocyanates on anhydrous cellulose in the presence of tertiary amines. They have few commercial applications; however, n-octadecyl and phenyl carbamates have been known for some years, the former being used to improve water repellency of fabrics (Hamalainene et al., 1954).

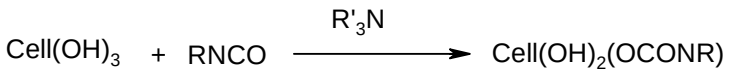

4. Sulfonates

Cellulose can be esterified with organic sulfonyl chlorides in the presence of tertiary amines or alkali hydroxides (Fisher, 1959). Most of the work has been done using p–toluenesulfonyl (tosyl) chloride, methane sulfonyl (mesyl) chloride, and benzene sulfonyl chloride. A comparatively stable cellulose ester is formed which has no affinity for direct dyes. Yarns treated in this manner remain white when dyed and when blended with untreated cotton produce special effect yarn. The chemical properties of these esters have considerable preparative utility because of the reactivity of the substituents.

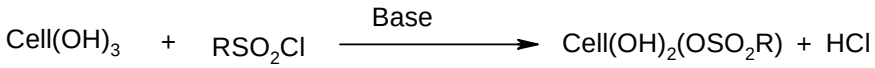

1.6.2.2 Inorganic Esters

1. Cellulose nitrate

Cellulose nitrate is the oldest cellulose derivative and the most important inorganic ester of cellulose. It finds applications in plastics, coatings, and explosives. The reaction (shown next page) is carried out by treating cellulose with nitric acid in the

presence of sulfuric acid and water (Green, 1963):

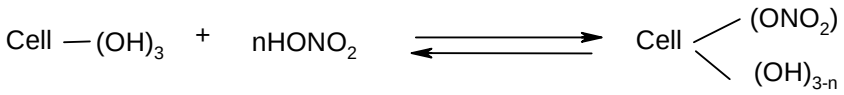

2. Cellulose sulfate

Sulfation of cellulose takes place by direct action of 70-75% aqueous sulfuric acid, followed by neutralization with a mild base to obtain a salt (Whistler and Spencer, 1963):

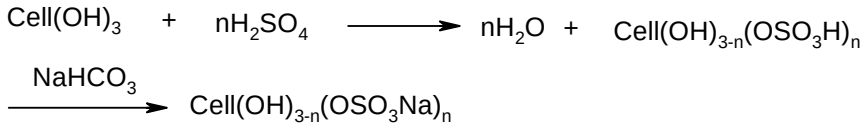

3. Phosphorous-containing cellulose derivatives

Cellulose phosphate esters of low phosphorus content can be prepared by the reaction of wood pulp or cotton linters with phosphoric acid in molten urea. However, higher phosphorus contents can be obtained with less degradation of the cellulose by using excess urea and short reaction times (15min) at high temperatures (140^0C). Reaction of cellulose with a mixture of phosphoric acid, phosphorus pentoxide, and an alcohol diluent has been shown to produce a stable, water-soluble cellulose phosphate with high degree of substitution (Touey, 1956).

1.6.3 New Cellulose Esters

New cellulose esters were prepared using new reagents and /or organic cellulose solvent systems. Cellulose esters containing relatively long aliphatic chains were prepared with fatty acid chloride and pyridine under heterogeneous solid-liquid phase conditions, and their liquid crystalline properties were studied (Itoh et al., 1992).

Fluorine-containing polymers have unique thermal resistance, water and oil repellency, small dielectric constant, and piezoelectric properties. Introduction of fluorine-containing groups through ester linkage into cellulose backbone has been investigated (Isogai, 2000). Some fluorine-containing cellulose esters are listed in Fig.1-8.

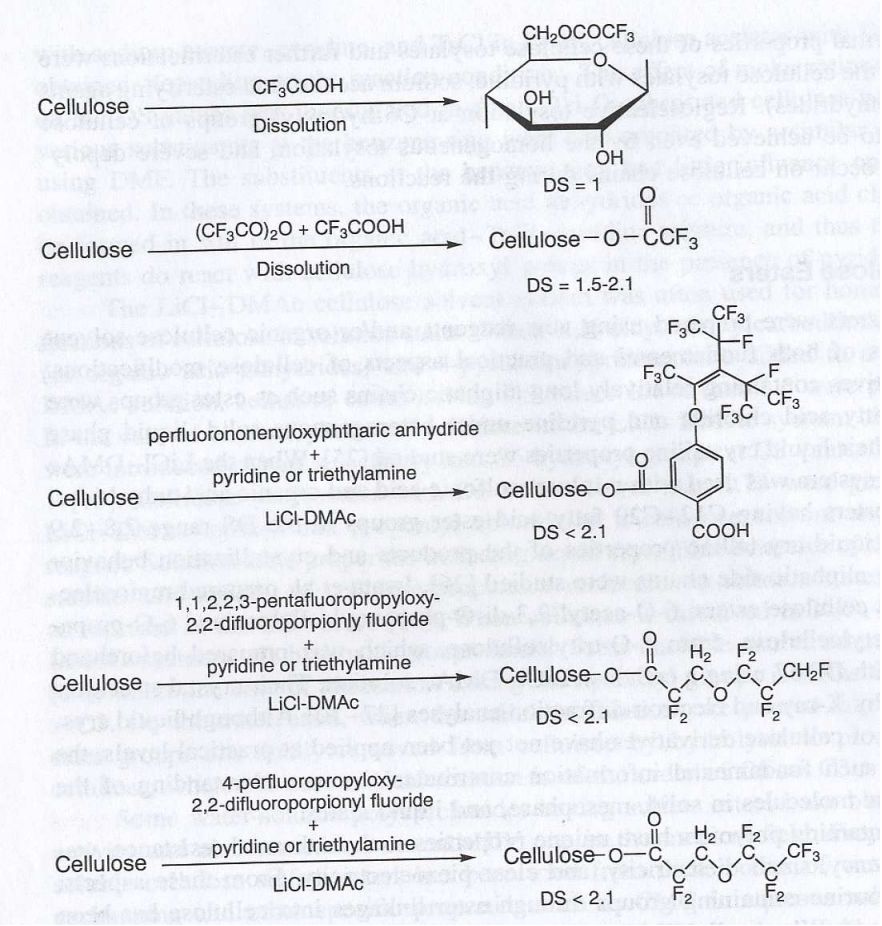

Figure 1-8*. Chemical structures of fluorine-containing cellulose esters.*

1.7 Etherification

Patents disclosing the preparation of cellulose ethers date back to the early 1900s (Lilienfeld, 1912 and 1916). Since that time, significant modifications of the processes and reactions involved have been made, and this area continues to be one of academic

and industrial research.

Two types of reaction are employed in the prepration of cellulose ethers. The most common is nucleophilic substitution. Methylation of alkali cellulose with a methyl halide (CH_3X) is an example of this type (the equations are shown below):

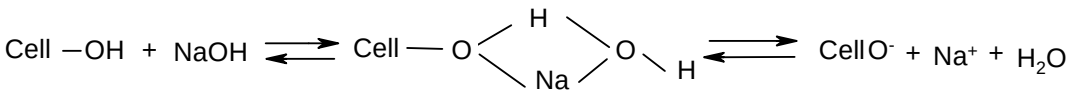

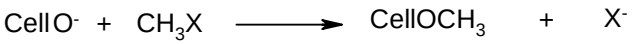

Preparation of hydrophobically modification water-soluble cellulose ether and characterization of their solution properties are the current topics for cellulose ethers. Some new cellulose ethers reported recently are illustrated in Figure 1-9 (Isogai, 2000).

1.7.1 Carboxymethylcellulose

Carboxymethylcellulose (CMC) is a polyelectrolyte with a pK_a of approximately 4, thus approaching the acid strength of acetic acid. It is usually marketed as the sodium salt, since its acid form has poor water solubility. Manufacturers are various and are found in most technologically advanced countries. Preparation of CMC was first patented in 1918(Jansen). Reactants have not changed significantly since then, although the preparation processes have. The use of alkaline aqueous organic slurry preparation has in many instances replaced the high-solids shredding procedures. Properly controlled slurry etherification generally results in a more uniform product.

The three possible positions for chemical derivatization in cellulose are the hydroxyl groups at C-2, C-3, and C-6. Experimentally determined molar distribution of carboxymethyl groups in CMC has been reported to be 2:1:2.5 for C-2, C-3, and C-6

hydroxyls. While the C-6 primary hydroxyl is generally thought to be most reactive in this particular system, this is not always so. There is considerable evidence that the C-2 hydroxyl group is the most acidic in cellulose. As a result, many equilibriums and rate-controlled reactions that involve cellulosic alkoxide ions appear to favor this site; exceptions are reactions in which steric hindrance is important. Recent NMR spectroscopic studies of substitution distribution indicate the following order: C-2>C-6>>C-3 (Parfondry and Perlin, 1977). The influence of reaction conditions on reactivity has also been studied (Gelman, 1982).

1.7.2 Hydroxyethylcellulose and hydroxypropycellulose

Hydroxyethycellulose is an important commercial product manufactured all over the word. Annual capacity had reached more than 85 million pounds by 1979 and was still expanding. The hydroxyethyl group has the constitution $–CH_2.CH_2OH$ Hydroxypropylcellulose is manufactured on a much smaller scale, mainly in United States. The hydroxypropyl group has the constitution $–CH_2.CH_2.CH_2OH$ (Nicholson and Merritt, 1985):

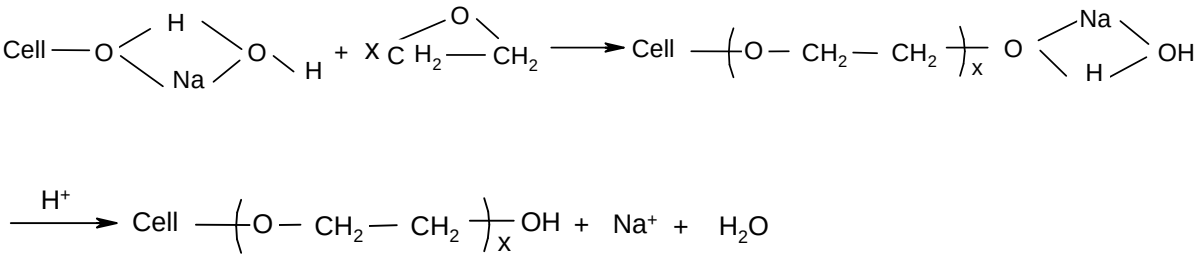

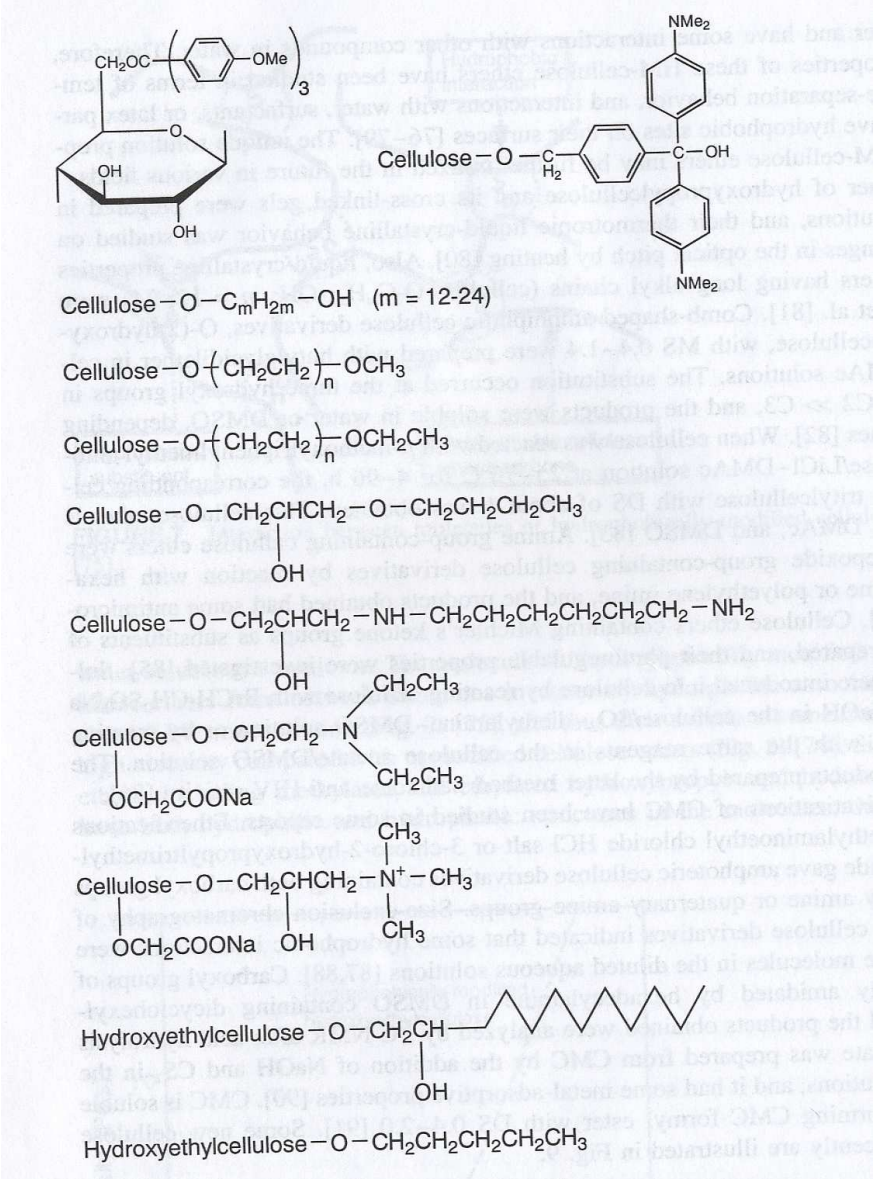

Figure 1-9. *Chemical structures of new cellulose ethers.*

1.7.3 Alkyl ethers of cellulose

The three most common and commercially important ethers in this class are methylcelllose, ethylcellulose and the mixed ether, hydroxyproplmethlycellulose. Methyl

and ethyl ethers os cellulose are prepared by the reaction of methyl and ethyl halides with alkali cellulose as described in section 15.1. Generally, commercial methylcellulose is water-soluble, and commercial ethylcellulose soluble in organic solvents. As discussed before, solubility varies with degree of substitution (DS).

The hydroxyalkylmethylcellulose is prepared by reaction of mixtures of methyl chloride and propylene oxide with alkali cellulose (Nicholson and Merritt, 1985) (the equations are shown below):

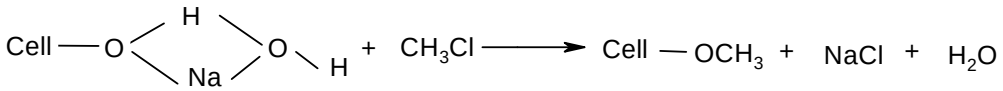

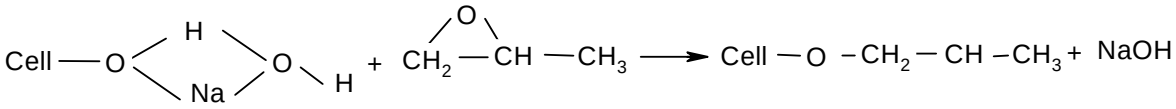

1.8 Grafting

In principle, all routes for polymer synthesis known today such as radical, ionic, and ring opening polymerization, polyaddition and polycondensation can be used for a covalent attachment of polymer side chains onto cellulose. In recent years, graft-polymerisation has been recognized as a simple and effective technique for introducing large quantities of desirable functional groups into a host substrate meanwhile the surface area of cellulose fiber is dramatically increased. Figure 1-10 and Figure 1-11 show the changes on the surface area of cellulose fibers before and after grafting. A considerable number of initiation methods are available and are generally based on ionizing radiation (Ranby, 1977), gamma radiation (Dilli et al., 1972; Guthrie and Haq, 1974), ultraviolet (Davis et al., 1977) and chemical reactions (Ranby, 1977).

In general, these have involved cationic or anionic grafts. These products have a large number of uses. As ion exchange materials, they are used for cleaning up textile waste water and for the recovery of precious metals and, in principle, for various air and water filtration and cleanup operations. They also can be used for binding enzymes and as bactericides when exchanged with certain metals or other entities (Stannett, 1985).

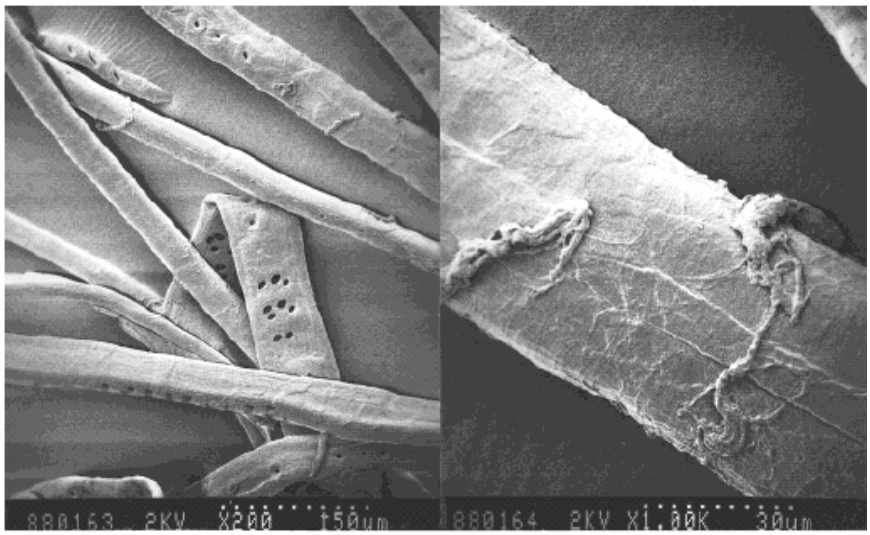

Figure 1-10. *Cellulose fiber before grafting.*

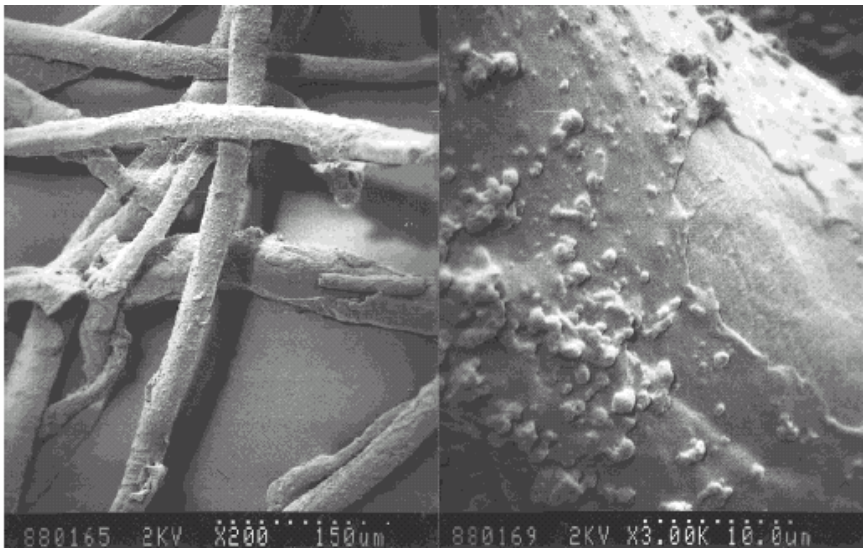

Figure 1-11. *Cellulose fiber after grafting*

1.9 Deoxyhalogenation

Preparation of cellulose derivatives that have C-X (X: halogen) groups have been studied often using nonaqueous cellulose solvent systems (Figure 1-12), and in some reports these deoxyhalogenated cellulose derivatives were further subjected to substitution reactions to add functionalities to cellulose (Isogai, 2000; Furuhata et al., 1992; Furuhata et al., 1995).

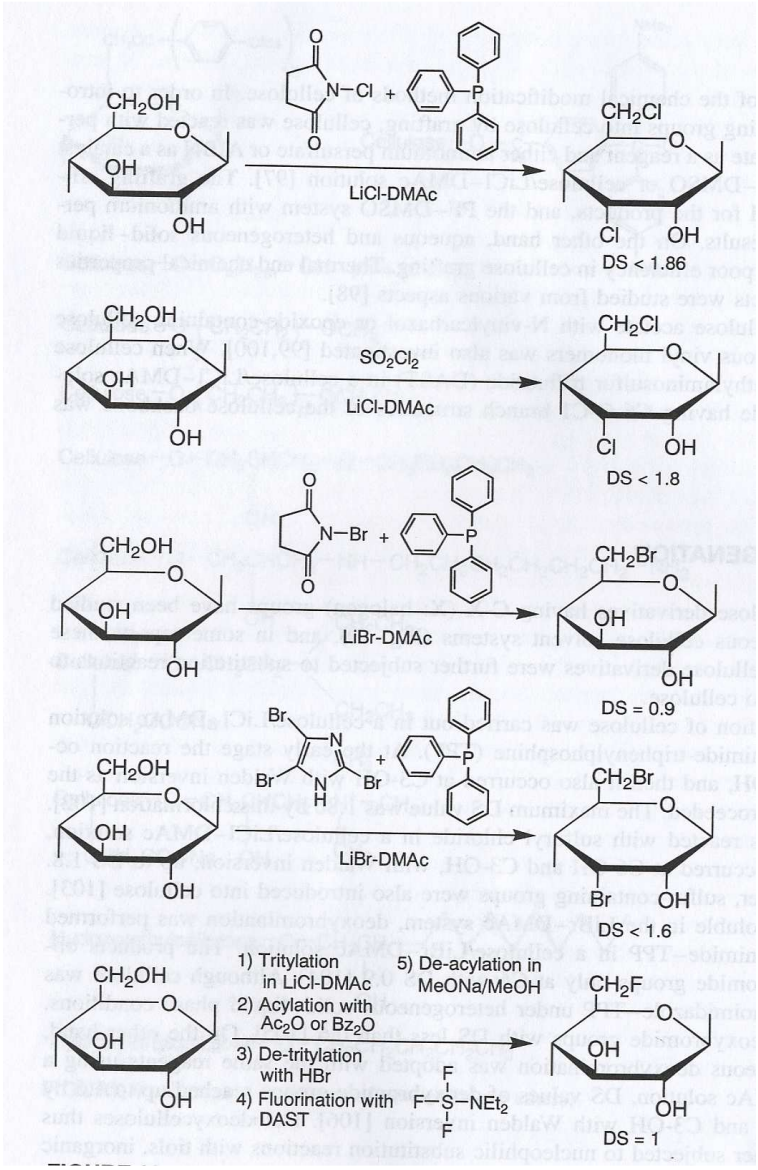

Figure 1-12. *Deoxyhalogenation of cellulose.*

1.10 Oxidation

Oxidation reactions applied to cellulose for chemical modifications in this decade are summarized in Figure 1-13.

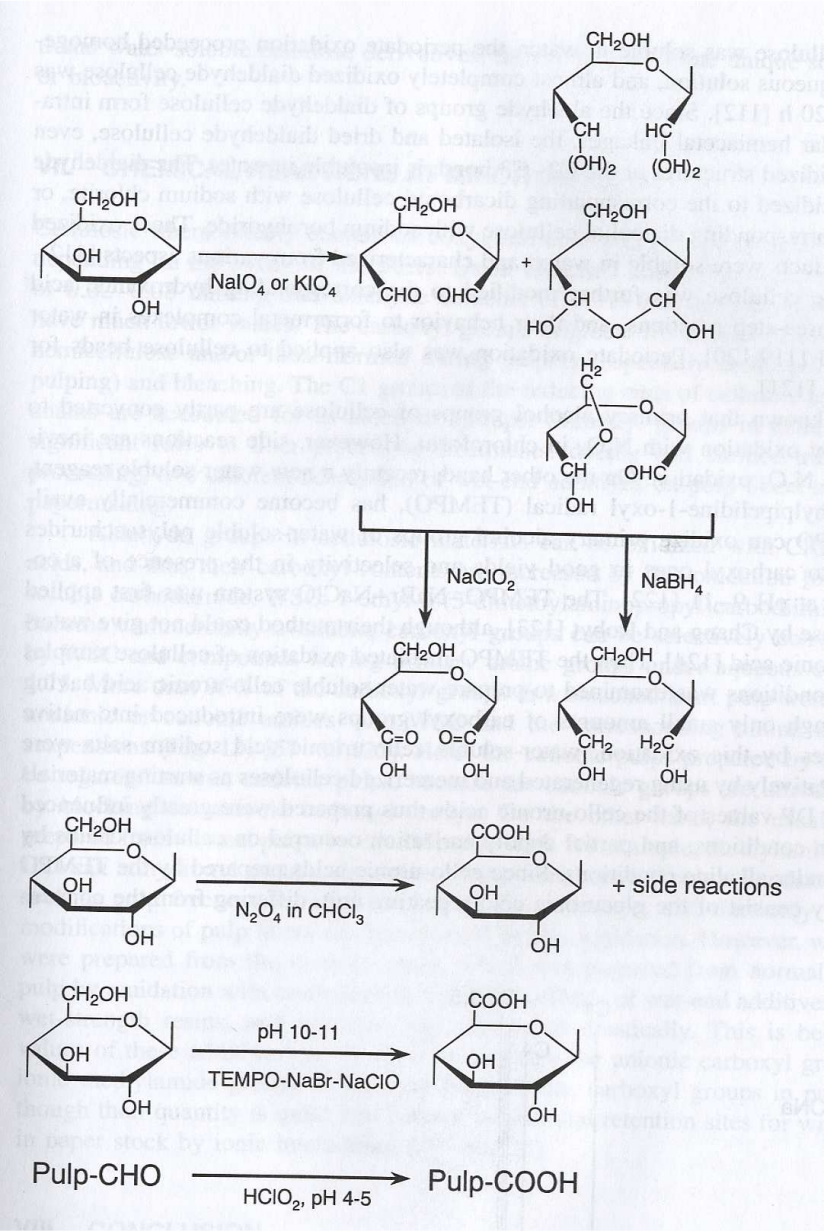

Figure 1-13. *Oxidation of cellulose.*

Some oxidation reactions occur on cellulose selectively at particular positions. The periodate oxidation is typically involved in this category, and has been used to

prepare dialdahyde cellulose at laboratory levels. Generally, the oxidation requires several days at room temperature in the dark to prepare dialdehyde cellulose from solid cellulose samples, whose C2 – C3 bonds are mostly cleaved. Thus, degrade of polymer is inevitable during the periodate oxidation (Morooka, et al., 1989; Varma and Chavan, 1995; Popa et al., 1996; Nevell and Zeronian, 1985).

1.11 An example of Anionic Ion Exchanger from Cellulose

Recently, researchers pay more attention to the application of sugarcane bagasse (BG) and rice hull (RH) as a raw material for producing anion exchangers. Pure cellulose (PC) and pure alkaline lignin (PL) were also used as reference materials to elucidate the reactivity of lignocellulosic agricultural waste materials (LCM). Although a large number of modification procedures for PL and PC have been reported in the literature, no chemical procedure to produce anion exchangers effectively from both materials has been developed (Funaoka et al., 1995; Hill and Mallon, 1998). The main objective of this study was to develop a new synthetic procedure to produce anion exchanger from LCM. Chemical modifications of BG, RH, PC and PL were conducted by reaction with epichlorohydrin and dimethylamine using pyridine as catalyst and *N*,*N*-dimethylformamide (DMF) as solvent.

Pyridine was used as a catalyst to open the strained three-membered ring of the epoxide group in weakly basic conditions (Morrison and Boyd, 1992). The nitrogen content of the final product was increased significantly from 0.6% to 4.80% by the increase in the reaction time with pyridine from 30 to 60 min. However, the nitrogen contents in the final product were almost the same (4.81%) between 60 and 120 min

showing that an hour of reaction was enough to expose all available hydroxyl groups in cellulose and to attach epichlorohydrin and dimethylamine. At reaction times of 60 and 120 min and in the presence of excess water in the reaction mixture, the nitrogen content was 0.3% and 0.35%, respectively. Nitrogen content was 0.36% in the absence of pyridine. This suggested that the reactions proceeded more efficiently in an organic medium. Hence, subsequent chemical treatment to convert LCM, PC and PL into anion exchangers was carried out without water and in the presence of the weak-base catalyst pyridine to increase the attachment of dimethylamine in the final products. Nitrogen content in the PC exchanger is known to indicate total amount of reactive sites in the exchanger (Ikeda et al., 1990).

Amino group incorporation into PC was decreased by the presence of water in the reaction mixture and increased with the reaction time and presence of a catalyst, pyridine. Bagasse and RH demonstrated maximum nitrate exchange capacities of 1.41 and 1.32 mmol/g, respectively, and yields of 412.5% and 180%, on the original material, respectively. Both lignocellulosic agricultural waste materials appeared to be potential materials to treat water contaminated with nitrate.

1.12 Two examples of Cationic Ion Exchanger from Cellulose

If negative charged functional groups are attached to the cellulose backbone, the cellulose will show the properties of positive abstraction. Then the cellulose becomes a cationic ion exchanger (Li, 2002 and Lehrfeld, 1996).

In the first case, Li and his colleagues propose the use of a commercially available, solid-state ion exchange membrane as an alternative to the binding phases currently used with

diffusive gradients in thin films (DGT) for the measurement of trace metal species. There are numerous such membranes currently available, made by the addition of electrophilic functional groups, such as phosphoric acid, carboxyl, amidoxime, hydroxamic acid and amidrazone hydrazide, to a backbone membrane structure, such as cellulose. Cellulose phosphate membranes, in particular, have been used for binding metal ions and for separation of trace metals. This material has excellent ion exchange properties combined with a desired hydrophilic nature. The binding functional groups, which are chemically immobilised on the cellulose backbone, provide good chemical stability and uniformity of coverage on all surfaces of the membrane. The excellent mechanical strength and flexibility of the material also makes it convenient for handling and preparation of the DGT assembly. Furthermore, the ion exchange properties of the membrane can easily be regenerated under acidic conditions to allow reuse of the material as a binding phase. The new binding phase exhibited excellent mechanical properties and overcame many of the problems of hydrogel-based binding phases including handling difficulty, fragility, ease of assembly and uniformity of binding sites.

In the second case, Lehrfeld (1996) prepared a series of cationic exchange resins from very low-value agricultural residues. In his investigation, carboxylate (maleate, succinate, and phthalate), phosphate, and sulfate group were incorporated onto the complex polysaccharide matrix of oat hulls, corn cobs, and sugar beet pulp (Figure 1-14). The order of reactivity was sugar beet pulp > corn cob > oat hull. Calcium ion binding capacities of these modified materials were measured, and some were additionally evaluated for their ability to remove lead from a standard water solution.

1.13 Research efforts on quaternized cellulose for color removal

Early studies involving addition of quaternary ammonium hydroxides to cellulose regarded quaternary ammonium as a swelling agent. This research did not continue primarily due to the high cost of the reagents (Toth et al., 2003). Recently such research has become popular again because the cost of tetramethylammonium hydroxide decreased and the applications of quaternized cellulose may increase.

Many studies have focused on the harvest agricultural residues as the adsorbents in order to reduce cost. A description of the performance characteristics of an ideal dye adsorbent would be to have high capacity and rapid binding kinetics, to be easily and inexpensively regenerated (Laszlo, 1994; Rock and Stevens, 1975).

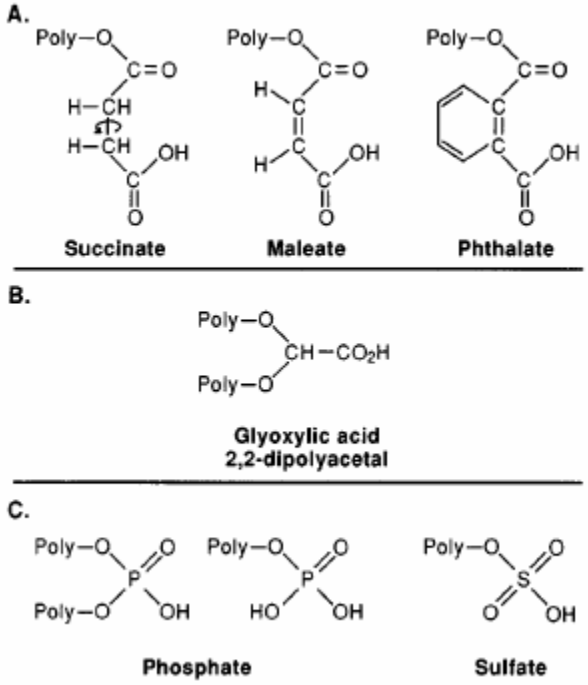

Figure 1-14. *A schematic depicting the special relationships of the functional groups grafted onto the polysaccharide backbone (Lehrfeld, 1996).*

Low cost of adsorbents can be prepared by quaternization of agricultural residue materials such as corn cob (Simkovic et al., 1992), surgarcane bagasse (Laszlo, 1996; Simkovic and Laszlo, 1997), soybean hull and sugar beet fiber (Laszlo, 1994), and sunflower stalk (Shi et al., 1999). The researches proved that quaterinized cellulose could be applied as an adsorbent in removal of both anionic and cationic dyes (Shi et al., 1999).

Because the bonding between quaternized cellulose and dyes involves coloumbic interactions, as well as inherent adsorption, the adsorbents can be regenerated by a simple salt plus base treatment without using organic solvents (Laszlo, 1995 and 1997, Jorgensen, 1979).

1.14 Summery

Due to the chemical and physical versatility of cellulose, many modification methods have been applied since a peak appeared in early 1950's (Rowell and Young). Cellulose as a polymer has been paid more and more attention because the high prices of oil based polymers. Research on the chemical modification of cellulose has been successful in expanding and maintaining the use of cellulose on textile industry, environmental industry, and biological industry.

1.15 References

Blackwell, J.; Marchessault, R. H. In *Cellulose and cellulose derivatives*; Bikales, N.; Segal L. E., Eds.; Wiley-Interscience: New York, 1971.

Budd, J.; Herrington, T. M. *Colloids and Surfaces* **1989**, *36*, 273-288.

Campbell, W. H. http://www.bio.mtu.edu/campbell/482w61.htm, 1996.

Davis, N. P.; Garnett, J. L. *Modified Cellulosics*, Academic: London, 1977, p197.

Davis, W. E.; Barry, A. J.; Peterson, F. C.; King, A. J. *J. Am. Chem. Soc.* **1943**, *65*, 1294-1300.

Dilli, S.; Garnett, J. L.; Martin, E. C.; Phuoc, D. H. *J. Polym. Sci.* **1972**, *C37*, 57.

Fardim, P.; Duran, N. *Colloids and Surfaces, A: Physicochem. Eng. Aspects*, **2003**, *233*, 263-276.

Felix, J. M.; Gatenholm, P. *Nordic Pulp and Paper Research Journal*, **1993**, *1*, 200-203.

Fisher, J. W. in *Recent Advances in the Chemistry of Cellulose and Starch*, Honeyman, J. Ed.; Heywood: London, 1959, p188.

Funaoka, M.; Matsubara, M.; Seki, N.; Fukatsu, S. *Biotech. Bioeng.* **1995**, *46*, 6.

Furuhata, K.; Chang, H. –S.; Aoki, N.; Sakamoto, M. *Carbohydr. Res.* **1992**, *230*, 151

Furuhata, K.; Aoki, N.; Suzuki, S.; Sakamoto, M. *Carbohydr. Polym.* **1995**, *26*, 25.

German, R. A. *J. Appl. Polymer. Sci.*, **1982**, *27*, 2975.

Green, J. W. in Methods in *Carbohydrate Chemistry*; Whilster, R. L. Ed.; Academic: New York and London, 1963; Vol. 3, pp 213-217.

Gurnagul, N.; Gray, D. G. *Journal of Pulp and Paper Science* **1985**, *11* (4), 98-101.

Guthrie, J. T.; Haq, Z. *Polymer* **1974**, *15*, 133.

Hamalainen, C.; Reid, D.; Berard, N. *Dyestuff Report* **1954**, *43*, 457

Hayashi, J.; Kon, H.; Takai, M.; Hatano, M.; Nozawa, T. in *The Structure of Cellulose*, Atalla, R. H. Ed.; American Chemical Society: Washington, DC, 1987, pp 135-150.

Hayashi, J.; Sufoka, A.; Ohkita, J.; Watanabe, S. *J. Polymer Sci.: Polymer Letters Edition* **1975**, *13*, 23-27.
Heize, T.; Liebert, T. *Progress in Polym. Sci.* **2001**, *26*, 1689-1762.

Hermans, P. H.; de Booys, J.; Maan, J. *Kolloid-Zt.* **1943**, *102*, 169.

Hermans, P. H.; Weidinger, A. *J. Appl. Polym. Sci.* **1948**, *11*, 1027

Hermans, P. H.; Weidinger, A. *J. Polym. Sci*, **1949**, *4*, 709

Hill, C.; Mallon, S. *Holzsforchung* **1998**, *52*, 427.

Hon, DN-S. in Chemical modification of cellulose; Hon, DN-S., Ed.; Marcel Dekker: New York, Basel, Hong Kong, 1996; p 114

Ikeda, I.; Hitoshi, T.; Kamihiro, S. *Sen'I Gakkaishi* **1990**, *46* (2), 63–68.

Isogai, A. in Wood and Cellulose Chemistry. Hon, DN-S. Ed.; Marcel Dekker: New York, 2000; pp 599-625.

Itoh, T.; Tsuji, T.; Suzuki, H.; Fukuda, T.; Miyamoto, T. *Plymer J.* **1992**, *24*, 641.

Jansen, E. German Patent 332,203, 1918.

Jeffries, R.; Roberts, J. G.; Robinson, R. M. *Textile Res. J.* **1968**, *38*, 234-224.

Jones, D. W. *J. Polym. Sci.* **1958**, *32*, 371.

Jorgensen, S. E. *Water Res.* **1979**, *13*, 1239-1247.

Kennedy, J. F.; Phillips, G. O.; Wedlock, D. J.; Williams, P. A. in *Cellulose and Its Derivatives*; Ellis Ed.; Horwood: England, 1985; p 12

Laszlo, J. A.; Dintzis, F. R. *J. Appl. Polym. Sci.* **1994**, *52*, 531-538.

Laszlo, J. A. *Am. Dyest. Rep.* **1994**, *83* (3), 17-21.

Laszlo, J. A. *Text. Chem. Colori.* **1995**, *21* (4), 25-27.

Laszlo, J. A. *Text. Chem. Colori.* **1996**, *28* (5), 13-17.

Lehrfeld, J. *J. Appl. Polym. Sci.* **1996**, *61* (12), 2099-2105.

Li, G.; Shen, J. *J. Appl. Polym. Sci*. **2000**, *78*, 676.

Lilienfield, L. British Patent 12,854, 1912.

Lilienfield, L. US Patent 1,188,376, 1916.

Marchessault, R. H.; Sarko, A. in *Advanced Carbohydrate Chemistry 22*; Wolfrom, M. L. Ed.; Academic: New York, 1967; pp 421-483.

Marchessault, R. H. and Sundararajan, P. R. in Cellulose; Academic: New York, 1983; p 11.

Marrinan, M.; Mann, J. *J. Polymer Sci.* **1956**, *21*, 301-311.

Martin M. J.; Artola A.; Balaguer M. D.; Rigola M. *Chem. Eng. J.* **2003**, *94*, 231–239.

Morooka, T.; Norimoto, M.; Yamada, T. *J. Appl. Polym. Sci.* **1989**, *38*, 849.

Morrison, R. T.; Boyd, R. N. *Organic Chemistry*, 6th ed.; Prentice-Hall International Editions: New York University, 1992.

Nicholson, M. D.; Merritt, F. M. in *Cellulose Chemistry and Its Applications*; Nevell, T. P.; Zeronian, S. H. Eds.; Ellis Horwood: Great Britain, 1985; pp 362-379.

Nevell T. P. and Zeronian, S.H. *Cellulose Chemistry and Its Applications*; Ellis Horwood: Great Britain, 1985; p 27 and pp 344-380.

Nevell, T. P. *Cellulose Chemistry and its Applications*; Ellis Horwood: West Sussex, England, 1985; p 241.

Odberg, L., Tanaka, T.; Swerin, A. *Nord. Pulp Paper Res. J.* **1993**, *8* (1), 6.

O'sukkivan, A. C. *Cellulose* **1997**, *4*, 173-207.

Parfondry, A.; Perlin, A. S. *Carbohydr.* Res., **1977**, *57*, 39.

Popa, M. I.; Aelenei, N.; Ionescu, G. *Cellulose Chem. Technol.* **1996**, *30*, 33.

Ranby, B. *Modified Cellulosics*; Academic: London, 1977; p 171.

Ratte, I. D.; Breuer, M. M. *The physical chemistry of dye adsorption*; Academic: London and New York, 1974; pp 2-14.

Rock, S. L.; Stevens, B. W. *Text. Chem. Colori.* **1975**, *7* (9), 169.

Rowland, S. P. in Modified Cellulose; Rowell Ed.; Academic: New York, 1978; pp 147-

170.

Sarko, A. in *Wood and Cellulosics: Industrial utilization, biotechnology, structure and properties*; Kennedy, J. F. Ed.; Ellis Horwood: Manchester, UK 1987; pp 55-70.

Shen, W.; Sheng, Y. J.; Parker, I. H. in *Cellulosic Pulps, Fibers and Materials*; Kennedy Ed. Woodhead: Cambridge, London, 2000; pp 181-196.

Shi, W., Xu, X. and Sun, G. *J. Appl. Polym. Sci.* **1999**, *71*, 1841-1850

Simkovic, I.; Mlynar, J.; Alfoldi, J. *Carbohydr. Polymer* **1992**, *17*, 285-288.

Simkovic, I.; Laszlo, J. A. *J. Appl. Polym. Sci*. **1997**, *64*, 2561-2566.

Stana-Kleinschek, K.; Kreze, T.; Ribitsch, V.; Strnad, S. *Colloids and Surfaces A: Physicochemical and Engineering Aspects* **2001,** *195* (1-3), 275-284.

Stannett, V. T. *Cellulose and Its Derivatives*; John Wiley & Sons: New York, 1985; p 387.

Sugiyama, J.; Vuong, R.; Chanzy, H. *Macromolecules* **1991**, *24*, 4168-4175

Tanghe, L. J.; Genung, L.B.; Mench, J. W. *Methods in Carbohydrate Chemistry*; Whilster Ed.; Academic: New York, 1963; Vol. 3, pp 193-198.

Toth, T.; Brorsa, J.; Reicher, J. *Text. Res. J.* **2003**, *73* (3), 273-278.

Touey, G. P. US Patent 2,759,924 to Eastman Co., 1956.

VanderHart, D. L.; Atalla, R. H. *Macromolecules* **1991**, *24*, 4168-4175.

Varma, A. J.; Chavan, V. B. *Carbohydr. Polym.* **1995**, *27*, 63.

Wada, M.; Heux, L.; Sugiyama, J. *Biomacromolecules* **2004**, *5*, 1385-1391.

Wadsworth, L. C.; Cuculo, J. A. in *Modified Cellulose*; Rowell Ed.; Academic: New York, 1978; pp 117-146.

Whistler, R. L.; Spencer, W. W. *Methods in Carbohydrate Chemistry*; Whilster Ed.; Academic: New York, 1964; Vol. 3, p 265-267.

Zeronian, S. H. in *Cellulose Chemistry and Its Applications;* Nevell, Ed.; Ellis Horwood: Great Britain, 1985; pp 138-180.

CHAPTER 2

ANIONIC DYE DECOLORIZATION FROM TEXTILE WASTEWATER

2.1 Introduction

The decolorization of textile wastewaters is a major concern to which many diverse technologies have been applied with varying levels of success. Dyeing processes are now under continuing scrutiny in order to prevent or minimize harmful effects that may be attributed to any phase of wet textile processing. This is true in the case of anionic dyes (reactive, vat, sulfur, acid, direct, and azoic) on cellulosic fibers, as well as other fiber genera (nylon, etc.). There is a strong need for a “low cost” viable technology that can decolorize textile effluent. The processes for color removal from textile dye house effluents include technologies such as biological treatment (Fernando and Grant, 2003; Zissi et al., 2003), coagulation (Sanghi and Bhattacharya, 2003), adsorption (Sakkayawong et al., 2002), oxidation (Michielsen et al., 2002), and hyperfiltration (Gholami et al., 2003). Among these treatments, adsorption has attracted a considerable interest as a feasible procedure for removing color from the effluents (Ho and McKay 1998; McKay et al. 1999; Khatri and Singh, 2000). Activated carbon is the adsorbent most widely used for the removal of many organic contaminants which are biologically resistant, but it suffers two major drawbacks: it is prohibitively expensive and there are many technical problems connected with the regeneration of the polluted support. The carbon adsorption is slow and may pose hydraulic problems when used in packed beds

and when suspended solids are present (Montgomery, 1985; Weber, 1972).

In order to remain competitive, textile mills must find a treatment method that is very low cost in an environmentally benign manner. One discovery that offers significant potential for improving the speed and yield of dye removal in a non-polluting manner is the use of quaternary ammonium cellulose. Quaternary ammonium cellulose is made by the addition of compounds containing a quaternary ammonium group capable forming an ether linkage to the cellulose molecule. Quaternization of cellulose (recycled newsprint) offers the potential of a large adsorption capacity and high speed for removing dye from wastewater at a very low cost. The objective of this research was to prepare a quaternary ammonium derivative of cellulose at room temperature using a no-salt, no-alkali dyeing process. Dye adsorption studies of these quaternized cellulose fibers are reported.

2.2 Experimental

2.2.1 Materials

The cellulose used in the experiments was recycled newspaper. Dyes used in the experiments were Direct Green 26 (C.I. 34045) from Organic Dyestuffs Corporation and Congo Red (C.I. 22120; FW: 696.67; content: 54%) from SIGMA Chemical Co. The quaternary ammonium compound, 3-chloro-2-hydroxy-N,N,N-trimethy-1-propanaminium chloride was supplied by The Dow Chemical Company and was used without further purification.

2.2.2 Pretreatment of Recycled Newsprint (Mercerized cellulose)

The recycled newsprint was treated with 18% sodium hydroxide (NaOH) at room temperature with vigorous stirring. The swollen cellulosic fibers were filtered and washed with distilled water until the pH was around 7.0. This product will serve as the treated

control sample designated as S1.

2.2.3 Pretreatment of Recycled Newsprint (Untreated cellulose)

Recycled newsprint was immersed in water for 24 hours, and then cut into very small pieces using a blender. The product was then filtered. This product will serve as the untreated control sample designated as S2.

2.2.4 Cellulose Quaternization Reaction (Cationization)

The cellulose quarenization reaction is divided into two steps. The first step of the quaternization reactions with cellulose, involves the conversion of the chlorohydrin form of the reagent into quaternary epoxy intermediate (2,3-epoxypropyltrimethyl-ammonium chloride, FW: 188) shown in Figure 2-1.

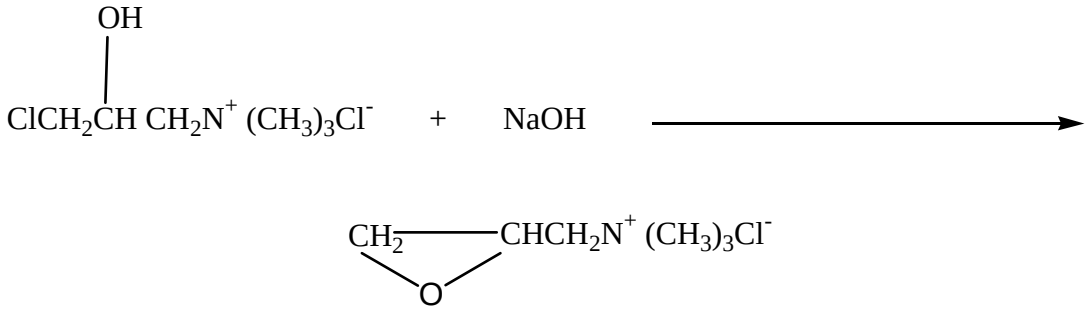

Figure 2-1. *Conversion of the Quaternary Chlorohydrin to the Epoxy Form.*

Next, the quaternary epoxy intermediate (FW: 151.5) reacts with the –OH group on the cellulose polymer at the C-6 position to form the quaternized cellulose fiber shown in Figure 2-2.

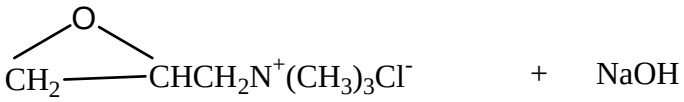

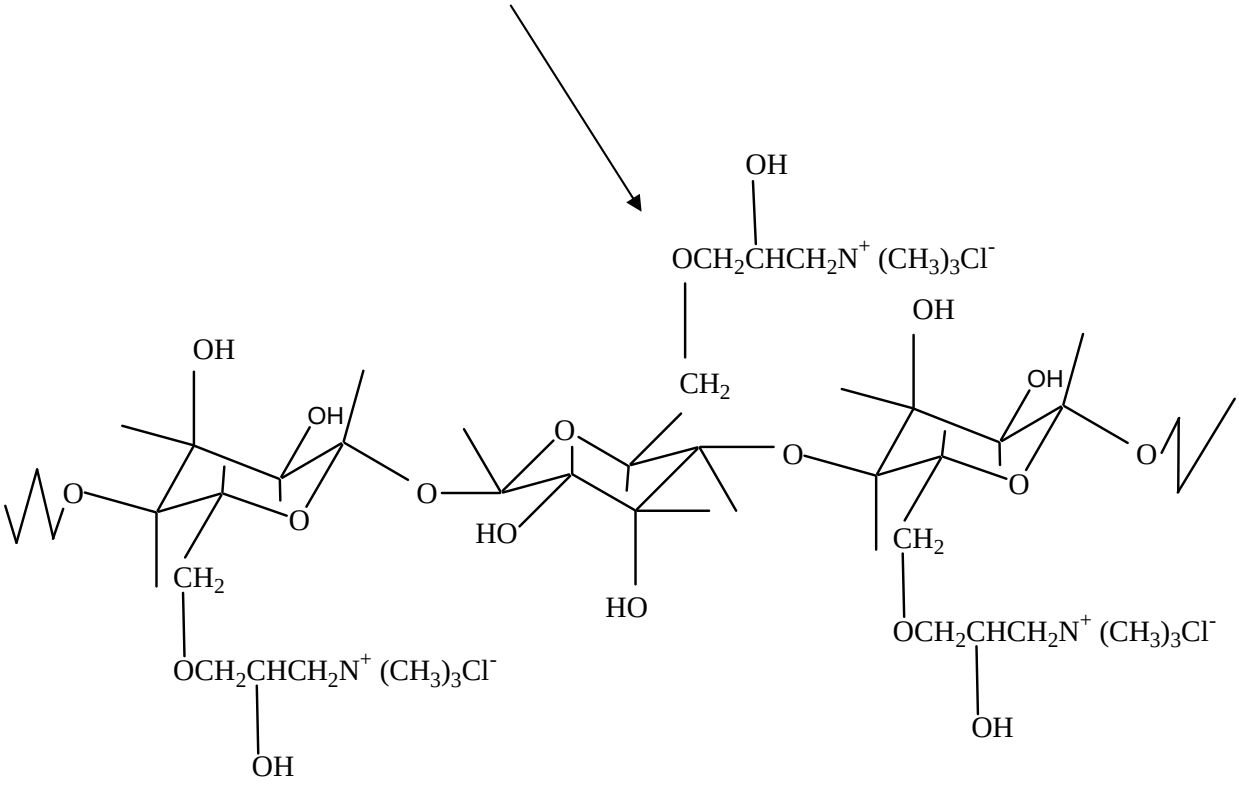

Figure 2-2. *Reaction of the Quaternary Epoxy with Cellulose fiber.*

2.2.5 Cationization: Method A:

Solution A was obtained by mixing 1 M quaternary ammonium and 1.1 M NaOH in order to convert the quaternary ammonium to the epoxy form at room temperature with vigorous stirring. Then 70 g of the mercerized cellulose was reacted with 250 g of the quaternary epoxy reactant (solution A) at room temperature with vigorous stirring, followed by addition of a concentrated NaOH solution to reach 4% of NaOH . The quaternized cellulose product (S3) was filtered and washed several times with distilled water. The similar procedures were used for other reactions designated as S4, S5, and S6 with some experimental changes. In the case of S4, a concentrated NaOH solution was

added to produce the quaternized cellulose product and the final concentration of NaOH was 6%. For S5 and S6, mercerized cellulose and untreated cellulose were reacted with quaternary epoxy without adding NaOH solutions.

2.2.6 Cationization: Method B*:*

Solution B resulted from mixing 2 M quaternary ammonium and 2.2 M NaOH in order to form an epoxy at room temperature under vigorous stirring. Then 70 g of the filtered mercerized cellulose was reacted with 250 g of the quat epoxy reactant (Solution B) at room temperature with vigorous stirring. Then, a concentrated NaOH solution was added to produce the quaternized cellulose product at a final concentration of NaOH of 8%. The product (S7) was filtered and washed several times with distilled water. The same procedures were used for other reaction designated as S8 with some experimental changes. With S8, no additional NaOH solution was added to the reaction mixture.

2.2.7 Effect of Quaternary Ammonium Concentrations on Nitrogen Contents

A quantity of mercerized cellulose was slurried with water and 30% NaOH was added to adjust pH to 12.5, then quaternary epoxy was added to the slurry in various amount: 5, 10, 15, 20, and 25% based on the weight of slurries (liquor ratio: 20:1). The epoxy quaternary was added drop wise to minimize hydrolysis. The reaction was allowed to stir for 1 hour at room temperature. The product was filtered and washed with distilled water several times until the pH was around 7. The names of samples are H1, H2, H3, H4, and H5 corresponding 5, 10, 15, 20, and 25% concentrations of epoxy quaternary.

2.2.8 Effect of pH conditions on Nitrogen Contents

A quantity of mercerized cellulose was slurried with water and 30% NaOH was added to adjust various pH, then quaternary epoxy was added to the slurry to form 10% quaternary epoxy at the final step (liquor ratio: 20:1). The quaternary epoxy was added

drop wise to minimize hydrolysis. The reaction was allowed to stir for 1 hour at room temperature. The product was filtered and washed with distilled water several times until the pH was around 7.

2.2.9 Nitrogen Analysis

Samples were dried at 45 ^{o}C under vacuum in a vacuum oven. The nitrogen contents were determined using a LECO CN-2000 instrument at 1050 ^{o}C. The analysis was performed at the Soil Test Lab of Auburn University.

2.2.10 Water Retention and Moisture Regain Tests

The water retention for each sample was measured on washed and filtered samples using the ASTM standard test method (Annual Book of ASTM Standards, D2404-94, 1998). Moisture regain was measured after the samples were dried using the ASTM standard test method (Annual Book of ASTM Standard, D4920-96b, 1998).

2.2.11 Precipitation Observation

Eight quaternized cellulose fiber samples were placed in eight 50 mL graduated cylinders containing 0.1% (0.005 g) Direct Green 26 dye solution at room temperature. The boundary between the dyed cellulose and the solution was observed. The scales of the high dyed cellulose were recorded after 12 hours.

2.2.12 Dye Removal Kinetics

The quaternized cellulose fiber was placed into 200 ml of dye solution containing 25 mg/L of Direct Red dye (C.I. 22120) at room temperature and stirred vigorously. The concentration of the dye in the solution at specific time intervals (every 1 minute for the first five points and every 5 minutes thereafter) was measured using a GeneSys 6 spectrophotometer (λ_{max} = 500 nm).

2.2.13 Dye Adsorption Isotherm

For the adsorption experiments, precisely weighed quaternized cellulose was placed in 50 mL Direct Red dye solution (C.I. 22120). The equilibrium isotherm experiments consisted of ten flasks containing the same amount of adsorbent, mixed with different concentration of dye solution. The liquor ratio is approximately 1:285. The dye solution concentration varied from 25 to 1000 mg/L of dye.

Each of the flasks containing quaternized cellulose fiber and dye solution was agitated in a constant temperature water bath at 25 ^{o}C. After 24 hours, the solution samples were filtered using a glass filter. The concentrations of the dye in the solutions ($[D]_s$) was measured using a GeneSys 6 spectrophotometer (λ_{max} = 500 nm) in order to calculate the amount of dye on the cellulose fibers ($[D]_f$). Then, the $[D]_s$ was plotted as a function of $[D]_f$.

2.3 Results and Discussion

2.3.1 Nitrogen Analysis

Table 2-1 summarizes the nitrogen analysis results under different reaction conditions. For samples S3, S4, S5, S6, S7, and S8, our preliminary results show that the percentage of nitrogen groups on the cellulose fibers overall depends on the concentration of sodium hydroxide (pH) and the concentration of the quaternary ammonium group in reaction solution (Rollins, 1997 and Hall 1996). However, the pretreatment does not affect on the nitrogen contents on the cellulose fibers based on the results of sample S5 and S6.

Table 2-1. Nitrogen analysis results under different conditions.

Sample #	Mercerized (18% NaOH)	Concentration of Quat (mol/L)	%NaOH in Reaction	% Nitrogen	Comments
S1	Yes	0		0.063	Control sample
S2	Water swelled only	0		0.075	Control sample
S3	Yes	1.0	4	1.33	
S4	Yes	1.0	6	1.21	
S5	Yes	1.0	0	0.26	
S6	Water swelled only	1.0	0	0.27	
S7	Yes	2.0	8	1.70	
S8	Yes	2.0	0	0.19	

2.3.2 Effects of Quaternary ammonium Concentrations and pH conditions on Nitrogen Contents

In order to reduce any byproduct formation and enhance the efficiency of the

reaction, a series of quaternary ammonium concentrations were prepared to determine the optimum reaction conditions. Figure 2-3 illustrates the effect of quaternary ammonium concentrations on the nitrogen contents on the cellulose fibers at a pH 12.5. The result shows that the percent nitrogen content on the cellulose fiber increased with increasing quaternary ammonium concentration when the quaternary ammonium concentration is less than 10%; but decreased beyond 10% oncetration, normally the hydrolysis process should increases with increasing liquor ratio and pH. It has been determined that the reaction of the quaternary ammonium with the cellulose does not occur until the pH is at least 11.5 (optimum at pH 12) (Rollins, 1997). The results of effects of pH conditions on the nitrogen contents shown in Figure 2-4 indicate that at a pH of 12.5, we were able to optimize the reaction conditions at 10% quaternary ammonium concentration. This concentration was calculated to be equivalent to the 1.0 mol/L of quaternary ammonium solution shown in Table 2-1.

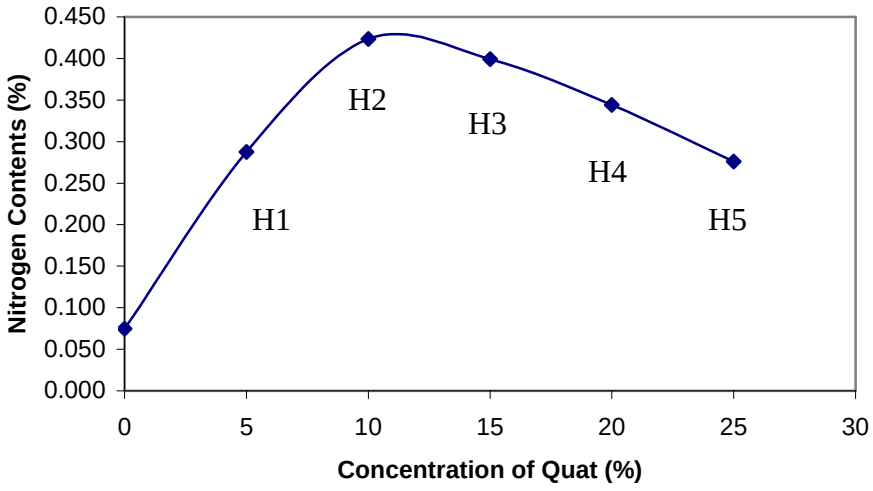

Figure 2-3. *The effect of quaternary ammonium concentrations on the nitrogen contents on the quaternized cellulose fibers.*

2.3.3 Water Retention and Moisture Regain

Water retention and moisture regain data for each sample are shown in Figure 2-5 and 2-6. In the reaction mixtures, the sodium hydroxide solution added can only swell the cellulose fibers in the amorphous regions but not in the crystalline regions. On the other hand, the quaternization occurred not only inside amorphous regions but also on the surfaces of the crystalline regions. The reaction resulted in increasing the polarity of cellulose fibers because a quaternary ammonium salt had been introduced into the chemical structures of cellulose fiber. This was proved by FT-IR data presented in the next chapter. Thus, both of the water retention and the moisture regain increased with increasing the percentage of nitrogen content in the fiber.

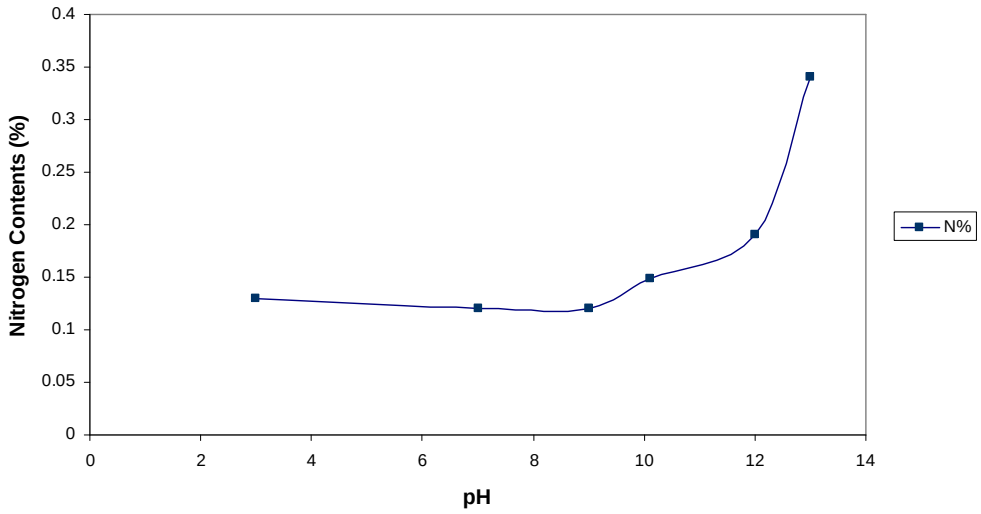

Figure 2-4. *The Effect of pH on the nitrogen contents at 10% quaternary ammonium.*

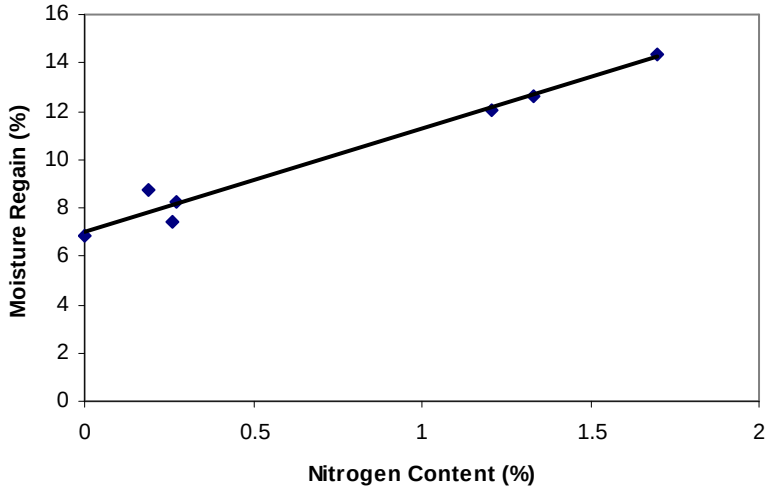

Figure 2-5. *The relationship between moisture regain and the nitrogen contents on the quaternized cellulose fibers.*

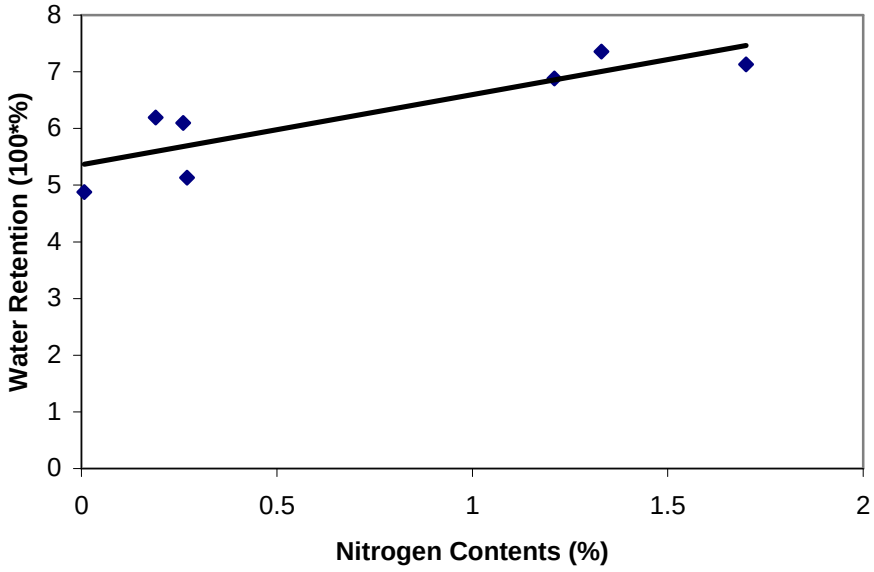

Figure 2-6. *The relationship between water retention and the nitrogen contents on the quaternized cellulose fibers.*

2.3.4 Precipitation Speed

The speed at which the quaternized cellulose fiber settles from slurries strongly depends on the nitrogen content or the dye adsorption tendency at certain dye concentration in solution. In Figure 2-7 sample S7 is shown to have the highest precipitation rate and on the contrary, a borderline has not been observed for sample S5, S1, and S2. The cellulose fibers become positively charged after the fibers are reacted with quaternary ammonium. Increasing nitrogen contents make the fiber possess a higher positive charge. As the positive charges increase, the fibers can adsorb more anionic dye from the dye solution and, consequently, the more the dye adsorbed on the fiber the easier it will be for it to precipitate from the solution.

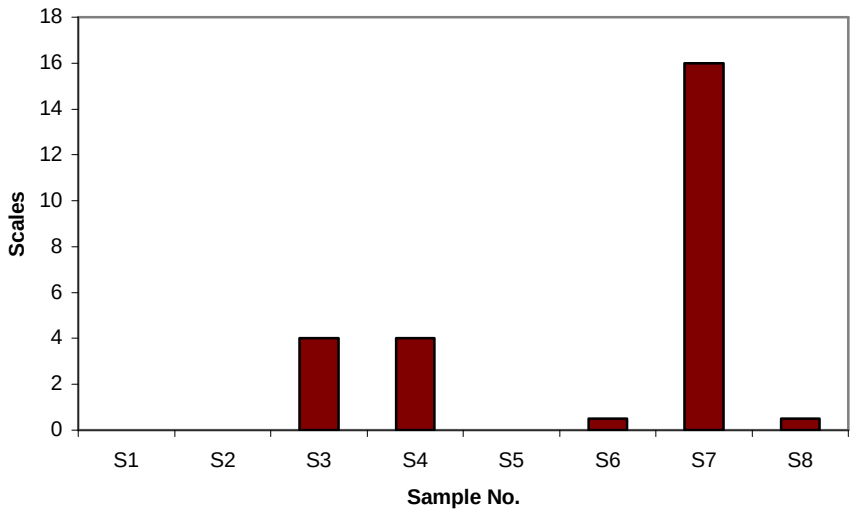

Figure 2-7*. The precipitation rate after 24 hour settling time.*

2.3.5 Dye Removal Kinetics

The dye removal speed is shown in Figure 2-8. The S1, control fiber has only been mercerized. The adsorption of dye by the S1 fiber occurs rapidly upon immersion in

the dye solution and reaches equilibrium within 3 min (dye concentration is 22 mg/L at equilibrium). However the solution remained a dark red color without dye being fully removed. The adsorption of dye solution for each of the S3 and S5 fibers occurred quickly within the first 1 minute. Both of the fibers adsorbed the dye solution at a similar rate, shown in Figure 2-8. Their rates remained constant for 25 min. There was a slight difference in their initial adsorption rates with the S5 fiber adsorbing (dye concentration is 2 mg/L at equilibrium) a little faster than the S3 fiber (dye concentration is 0 mg/l at equilibrium). The solution treated with the S3 fiber became clear after 1 minute upon immersion in the dye solution and the solution treated with the S5 fiber became a clear faint pink color (almost colorless) after 1 minute upon immersion in the dye solution. The adsorption of dye solution for the S7 fibers also occurred quickly within the first minute. However, the dye solution treated with the S7 fiber was still reddish after 25 minutes (dye concentration is 4 mg/L at equilibrium), even though the S7 fiber contained the highest nitrogen content. This phenomenon can be explained by the pore or channel model that is usually applied for natural fibers due to their fibrillar structures (Rattee and Breuer, 1974). Dye bonding sites are distributed on the surface of the pore or channel walls. The higher nitrogen contents could break the more hydrogen bonds in cellulose. This causes the cellulosic fibers to swell more (water retention can affect the structural changes) and then the pores or channels start to collapse, and thus the dye sites are difficult to be reached within a certain time. Therefore, the dye adsorption speed is controlled by a kinetic process. The dye adsorption speed is not only affected by the nitrogen contents, but also governed by the geometry of the pores and channels.

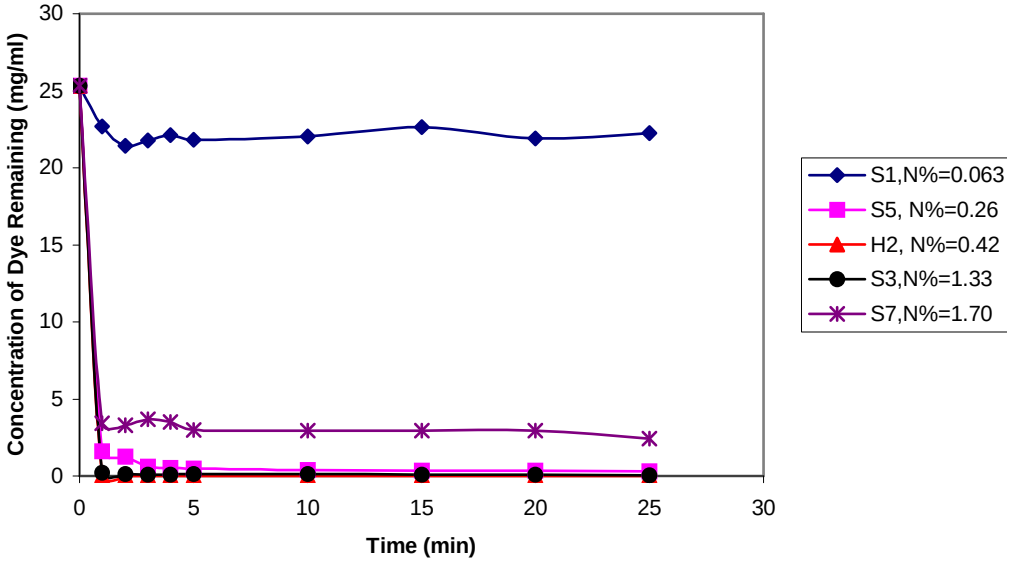

Figure 2-8. *The concentration of dye remaining in solution vs. time.*

2.3.6 Dyeing Adsorption Isotherm

The adsorption of concentrated dye solution in fibers with aqueous media, is a heterogeneous process, the following fundamental processes have to be considered: (a) diffusion of the dye into the polymer matrix; (b) adsorption on the surface; and (c) the adsorption which may or may not be followed by desorption. In the case of adsorption, there are two possible considerations: (1) adsorption without any interaction on with neighbors - Langmuir isotherm type and (2) adsorption involving the interaction between the neighbors – Freundlich and Temkin type or Brunauer, Emmett and Teller (BET) isotherm type (Rattee and Breuer, 1974). Only the Langmuir type will be discussed here. The Langmuir theory assumes that the adsorption happens in single layer and every available adsorptive site gets one dye molecule without interaction with its neighbors.

The adsorption curves in Figure 2-9, 2-11, and 2-13 indicate that the results obtained from the adsorption isotherm experiments can be explained using the Langmuir

isotherm models. This can be calculated using the following equation:

$$\text{The rate of adsorption} = V_a = k_1[D]_s([S] - [D]_f) \quad (2\text{-}1)$$

In which k_1 is the velocity constant of adsorption; $[D]_s$ is concentration of dye in solution at equilibrium; $[D]_f$ is concentration of dye on the fiber; [S] is saturation value of dye on fiber.

$$\text{The rate of desorption} = V_d = k_2[D]_f \quad (2\text{-}2)$$

In which k_2 is the velocity constant of desorption. At equilibrium the rates of absorption and desorption are equal so that:

$$V_a = V_d \quad (2\text{-}3)$$

$$k_1[D]_s([S] - [D]_f) = k_2[D]_f \quad (2\text{-}4)$$

let $K = k_1/k_2$,

$$[D]_f = K[D]_s([S] - [D]_f) \quad (2\text{-}5)$$

or $$[D]_f (1+K[D]_s) = K[D]_s[S] \quad (2\text{-}6)$$

Thus

$$\frac{1}{[D]_f} = \frac{1}{K[D]_s[S]} + \frac{1}{[S]} \quad (2\text{-}7)$$

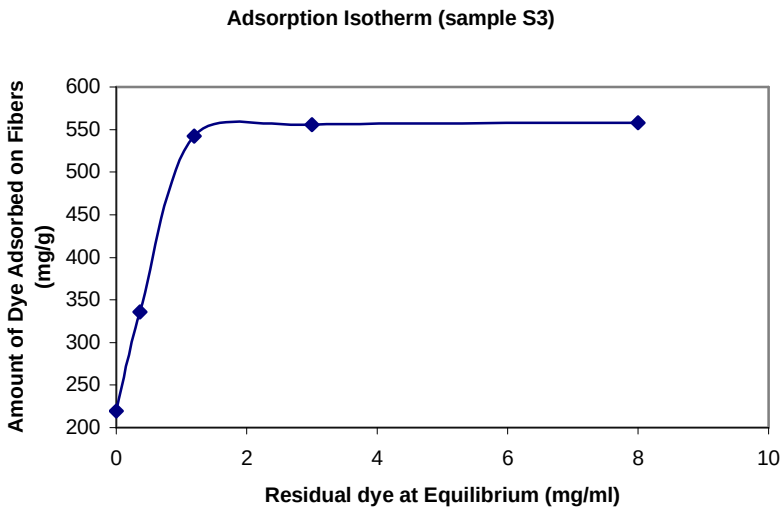

Figure 2-9. *Adsorption Isotherm of Sample S3.*

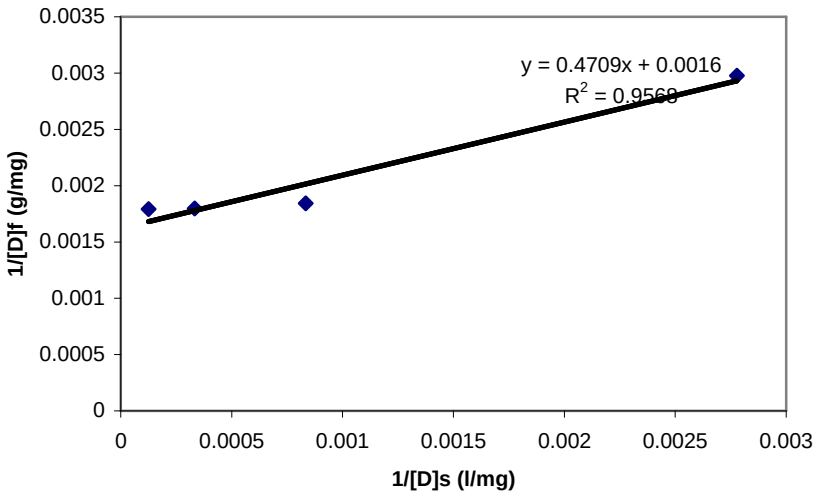

Figure 2-10. *Adsorption Isotherm of Sample S3.*

The interaction of the quaternary cellulose fiber with the dye solution was measured at 25^{o}C with a definite amount of the quaternized cellulose and with varying concentrations of dye solution from 25 up to 1000 mg/L until equilibrium was reached. The model was successfully applied to the adsorption isotherm of dye molecules onto the

quaternized cellulose fiber, where a Langmuir type of adsorption, involving saturation of the active surface sites does quantify the isotherm.

One should note the initial value of dye adsorbed on quaternized cellulose fiber, $[D]_f$ in Figure 2-9 and Figure 2-11. The values do not start at 0 mg/g of dye remaining in solution, instead it starts over 220 (mg/g) of dye remaining in solution. The reason for this is after 24 hrs of agitation, the amount of dye absorbed by the quaternized cellulose fiber for the first five dye solutions (remaining dye concentrations was less than 220 mg/g) were clear. Therefore, data collection began at 220mg/g of dye remaining in solution and higher. When the quaternized is reacted with the cellulose fiber, it becomes very highly positively charged. The attraction between the positive charges in fibers and negative charges in dye molecules makes the cellulose have a very high adsorption affinity toward the dye molecule, resulting in relatively strong adsorbent–adsorbate interactions. On the contrary, the untreated cellulose (Figure 2-11) and activated carbon do not posses such a strong positive charge, therefore the $[D]_f$ values are started at 0 (mg/g) with increasing dye concentrations (Martin et al., 2003).

The plot of $1/[D]_f$ vs. $1/[D]_s$ is given in Figure 2-10 and Figure 2-12 and is shown to be linear over the whole concentration range. The adsorption data yield a correlation coefficient greater than 0.96, and 0.99, for S1 and S3 fibers respectively, confirming an excellent fit to the Langmuir isotherm.

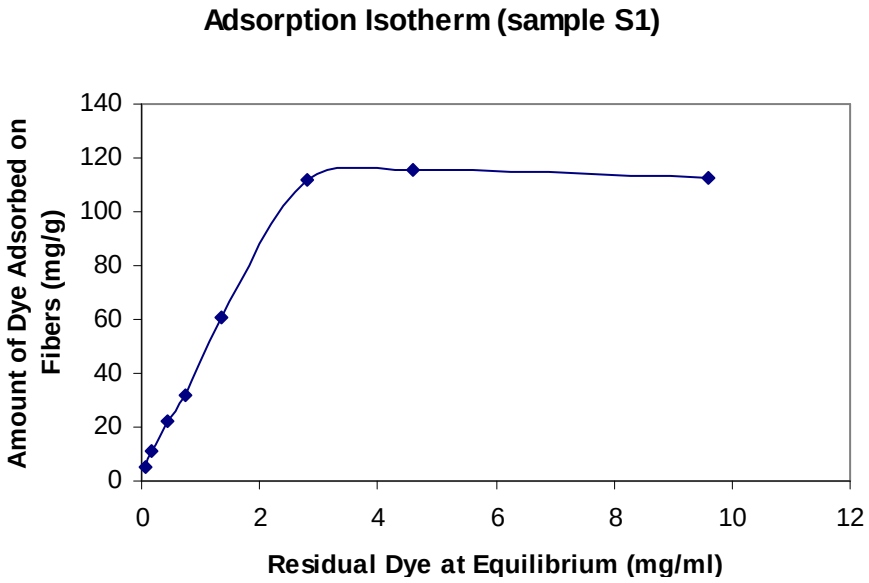

Figure 2-11. *Adsorption Isotherm of Sample S1.*

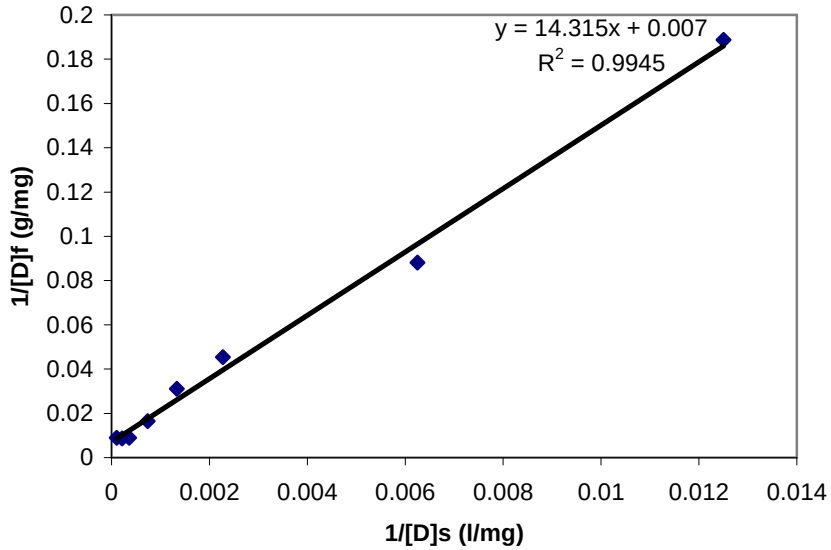

Figure 2-12. *Adsorption Isotherm of Sample S1.*

In the Table 2-2, the saturation values, [S], derived from the Langmuir isotherm model, are compared to that of the powdered activated carbon (Martin et al., 2003). As shown in Table 2-2, the sample of higher nitrogen content has a larger dye adsorption capability. The saturation values, [S], of quaternized cellulose are almost 10 times as high as that of the activated carbon. The greater dye adsorption capability is attributed to higher nitrogen contents or higher positive charges on the fibers. As mentioned before, the dye adsorptions of samples S1 and H2 are very fit the Langmuir model at lower nitrogen contents because the linear regressions are 1.00 and 0.99 respectively. However, the adsorption isotherm of sample S7 does not well fit the Langmuir model well because the linear regression of sample S7 is 0.72.

Table 2-2. Comparison of the parameters from fitting to Langmuir model with activated carbon.

Sample	[S] (mol/kg)	N%	R^2
S1	0.22	0.06	1.00
H2	0.35	0.42	0.99
S3	0.90	1.33	0.96
S7	0.96	1.70	0.72
Activated carbon (Martin et al, 2003)	0.07	0.17	1.00

In order to investigate the adsorption behavior of quaternized cellulose fiber, the molar numbers of adsorbed dye on the cellulose fiber and reacted quaternary group on the fiber can be calculated from Table 2-2. The results of the calculation are listed in Table 2-3. D and N represent the molar number of adsorbed dye on the fiber and the molar

number of quaternary group on the fiber respectively based on 1 kg of quaternized cellulose fibers. The proportion of D/N has an approximate value to 1 for sample H2 and sample S3 respectively. That means one molecule of quaternary group can bond one dye molecule at relative high nitrogen contents. This meets the assumption of Langmuir isotherm adsorption. On the other hand, the proportion of sample S7 is less than 1 and indicates the adsorption is not a monolayer adsorption. This is the reason that causes a poor linear regression of sample S7 shown in Table 2-2.

Table 2-3. The proportion of molar numbers of dye and nitrogen

Sample	Dye moles/kg (D)	Quat moles/kg (N)	D/N
H2	0.35	0.30	1.17
S3	0.90	0.95	0.95
S7	0.96	1.21	0.79

2.3.7 Relationship between Saturate Values and Nitrogen Contents

The saturation values of quaternized cellulose increase with the nitrogen contents due to the adsorption of the quaternized cellulose fits the Langmuir monolayer model at lower nitrogen contents. However, the saturation value levels off after the nitrogen content over is 1.5% shown in the Figure 2-13.

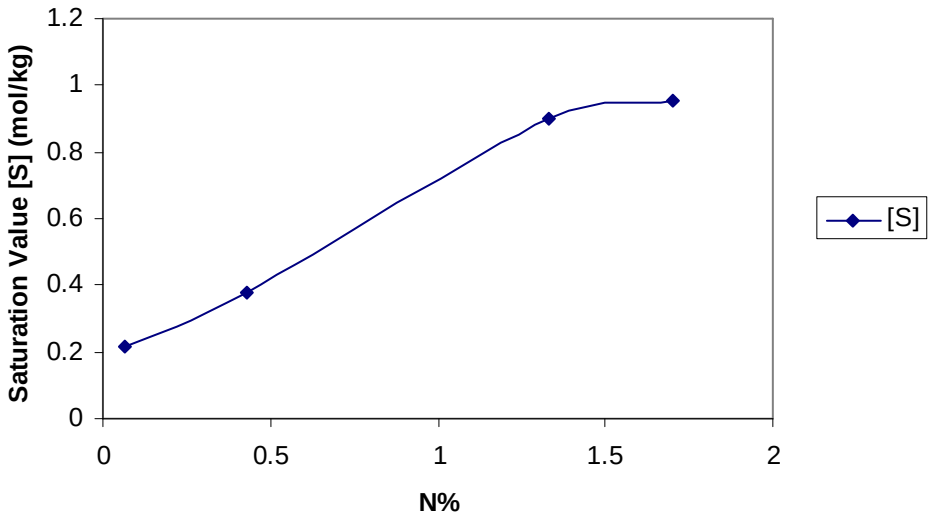

Figure 2-13. *The saturation values verse nitrogen contents.*

2.4 Conclusions

Any cellulose resources including recycled newsprint, straw, cardboard, hay (kudzu), and sawdust should posses an ability to act as a dye absorbent if they possess an extremely high anion dye adsorption capability after the cellulose is quaternized. The results of reacting cellulose (recycled newsprint) with quaternary ammonium groups indicate that the nitrogen contents depend greatly on the pH. The optimum pH is around 12. The alkali pretreatment is not important for cellulose to react with the quaternary epoxy. The quaternized cellulose of higher nitrogen contents possesses highest dye-adsorption capacity.

Increasing the amount of quaternary ammonium that react with the cellulose fibers, increases the number of dye bonding sites in the fiber. This is done by breaking up the hydrogen bonds between the polymer chains. This result in a more swollen

macrostructures and thus the dye molecules is able to get to the other dyes site available in the fiber. Therefore the dye removal kinetic does not only depend on the concentration of attached quaternary groups, but also on the number of dye sites available. It is also controlled by the number of dye site exposed to the dye molecular configuration inside the wall of the pores or the channels. The process of dye removal for quaternized cellulose can be completed within seconds when the concentration of the dye solution is less than 220 mg/L. The process of dye absorption fits the Langmuir model extremely well for S1 and S7 since the adsorption isotherm data according to Langmuir equation gave a linear plot over the whole concentration range. Thus the homogeneous monolayer adsorption process is significantly controlled by the dye bonding sites on the surfaces of the fibers and the surfaces on the walls of pores and channels inside fibers. The quaternized cellulose of higher nitrogen contents presents the higher saturation value of the dye. The saturation value of quaternized cellulose is more than 10 times higher than that of activated carbon. The quaternized cellulose fibers are shown to have an extremely high affinity for dye adsorption. These results show that the quaternized cellulose possesses very high capacity of dye adsorption in treating the textile dye wastewater.

2.5 References

Annual Book of ASTM Standards. Standard Test Method for Water Retention of Fibers (Centrifuge Method, D2402-94. 07.01), 1998; pp618-621.

Annual *Book of ASTM Standards*. Standard Terminology Relating to Moisture in Textiles, (D4920-96b. 07.02), 1998; pp 619-621.

Fernando, M. S; Grant, A. D. *Water Res.* **2003**, *37*(15), 3590-3601.

Garg, V. K.; Gupta, Renuka; B. Y. and Kumar, R. *Bioresource Tech.* **2003**, *89*(2), 121-124.

Gholami, M.; Nasseri, S.; Alizadehfard, M.R.; Mesdaghinia, A. *Water Quality Res. J. Can.* **2003**, *38*(2), 379-391.

Hall, D.M. US Patent 5,489,313, 1996.

Ho, Y. S.; McKay G. *Process Safety Environ. Protect* **1998**, *76*, 313-318.

Khatri, S. D.; Dingh M. K. *Water Air Soil Pollut.* **2000**, *114*, 423-438.

Martin, M. J.; Artola, A.; Balaguer, M. D.; Rigola M. *Chem. Eng. J.* **2003**, *94*, 231–239

McKay, G.; Porter, J. F.; Prasad, G. R. *Water Air Soil Pollut.* **1999**, *114*, 423-438.

Michielsen, S.; Bottomley, L.; Stojiljkovic, I.; Thompson, K.; Montgomery, C.; Bozja, J. National Textile Center Annual Report M01-GT01; Willington, DE, November, 2002.

Montgomery, J. *Water treatment principles and design*; J. Wiley and Sons: New York, 1985.

Rattee, I. D.; Breuer M. M. *The physical chemistry of dye adsorption*; Academic: London and New York, 1974; p86-91.

Rollins, C. K. Master of Science thesis, Auburn University, 1997.

Sakkayawong, N.; Thiravetyan, P.; Nakbanpote, W. *Advances in Chitin Sci.* **2002**, *5*, 568-575.

Sanghi, R.; Bhattacharya, B. *Water Quality Res. J. Can.* **2003**, *38*(3), 553-562.

Weber, W. *Physicochemical processes for water quality control*; J. Wiley and Sons: New York, 1972.

Zissi, L. S.; Kornaros, U.; Lyberatos, G. *Chem. Eng. Commun.* **2003**, *190*(5-8), 645-661.

CHAPTER 3

THE CHARACTERIZATION OF THE SURFACETHERMODYNAMICS OF QUATERNIZED CELLULOSE FIBER BY INVERSE GAS CHROMATOGRAPHY

3.1 Introduction

Cellulosic materials, as an ionic exchange precursor, are particularly attractive because cellulose is the richest resource of naturally occurring polymers on the earth. The chemical structure, composition, and surpermolecular structures of cellulose determine its chemical and physical properties. The surface properties of cellulose or chemically modified cellulose used as an ionic exchanger are extremely important. Inverse gas chromatography (IGC) as a very useful tool has frequently been applied for the evaluation of surface characteristics of cellulose and modified cellulose (Gurnagul and Gray, 1985; Felix and Gatenholm, 1993; Belgacem et al., 1996; Tshabalala, 1997; Papirer et al., 2000; Santos et al., 2001; Voelkel, 2004). It has become an accurate, reliable and rapid method for the physicochemical characterization of polymers and their blends, fibers, and other surfaces or surfactants.

The surface energetics and acid-base characteristics of cellulose were investigated according to Gutmann's electron acceptor-donor approach (Felix and Gatenholm, 1993; Shen and Parker, 2000). This method is a powerful tool to evaluate the filtration properties of nonwoven fabrics because the filtration is related to the physicochemical phenomenon on the surfaces of the fibers.

The work described in the previous chapter and the most of the researches on quaternized cellulose have been done on a lab scale and none of these studies provide

insight about the adsorption mechanisms particularly the surfaces properties of the crystalline or amorphous structures.

The thermodynamic work of adhesion is directly related to intermolecular interactions that can be split into dispersive and specific components (Mukhopadhyay et al., 1995):

$$W = W^{D} + W^{SP} \qquad [3\text{-}1]$$

where W is work of adhesion or adsorption, D is dispersive interaction, and SP is specific interactions like H-bonding, acid-base, and polar interactions.

The term “inverse” derives from the fact that IGC does not characterize the injected probe, as in traditional GC, but instead the stationary phase in the column. Experiments yield the residence time in the column of a certain defined probe. This residence time, or net retention time in an IGC column, appears in the following equation for calculation of the net retention volume:

$$V_N = JF(t_r - t_0) \qquad [3\text{-}2]$$

where V_N is the net retention volume, F is the carrier gas flow rate, t_r is the retention time of the probe, t_0 is the zero retention reference time, dead time (methane), J is the James-Martin correction, which corrects the retention time for the pressure drop in the column bed (Reutenauer and Thielmann, 2003)

When IGC measurements are carried out at infinite dilution, the free energy of adsorption per mole of probe, ΔG_{ads} (Schultz and Lavielle, 1989; Flix and Gatenholm, 1993; Shen and Parker, 1999) is given by:

$$\Delta G_{ads} = -RT\ln V_N + C \qquad [3\text{-}3]$$

where V_N is the net retention volume of the probe, C is a constant; R and T are the gas constant and temperature, respectively. Assuming that the free energy of adsorption due to dispersive and specific (acid-base) interactions are additive, a new equation can be derived (Riedl and Kamdem, 1992; Schultz and Lavielle, 1989):

$$-RT\ln V_N + C = \Delta G_{ads}^{D} + \Delta G_{ads}^{SP} \qquad [3\text{-}4]$$

Dorris and Gray (1980) proposed that the key link between the change in free energy of adsorption and the work of adhesion is given by:

$$\Delta G_{ads} = -N \cdot a \cdot W \qquad [3\text{-}5]$$

where N is Avogadro's number, a is the surface area of the adsorbate molecular (the probe). When dispersive interaction is only considered ($W^{SP} = 0$), the specific dispersive surface free energy of adsorption can be written as

$$W = W^{D} = 2Na\sqrt{r_L^D}\ \sqrt{r_S^D} \qquad [3\text{-}6]$$

After combination of [3-4], [3-5], and [3-6], then we get:

$$RT\ \mathrm{Ln}(V_N) = 2N(\gamma_S^D)^{1/2} \bullet a(\gamma_L^D)^{1/2} + C \qquad [3\text{-}7]$$

where γ_S^D is the dispersive component of the surface energy of adsorbent (cellulose fiber), γ_L^D is the dispersive component of the surface energy of adsorbate (the probe), and C is a constant.

The dispersive component of the surface energy of adsorbent (γ_S^D) describes the potential of cellulose to exchange London type interactions. From a plot of the free energy of adsorption of liquid probes onto solids ($RT\ln V_N$) as a function of the γ_L^D, a straight line is obtained. The dispersive component of the solid surface energy is then obtained from the slope of this line (see Figure 3-1).

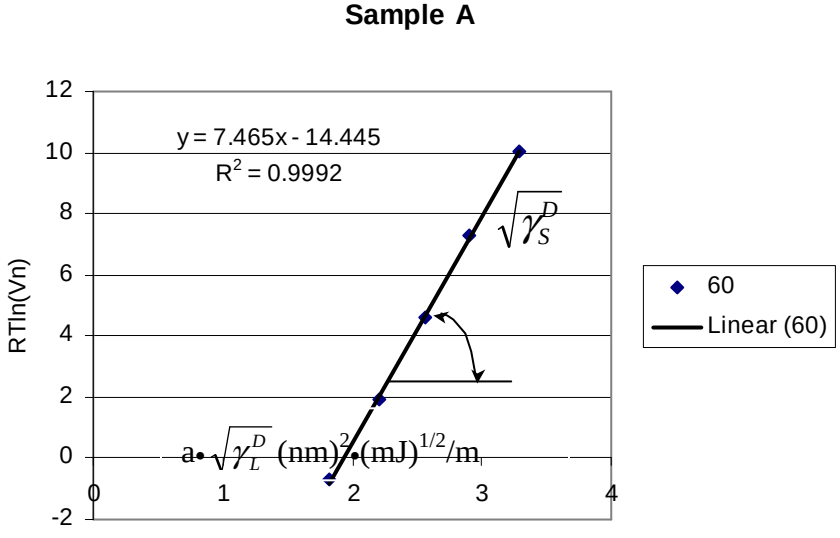

Figure 3-1. *Variati*
*2N*a* $\sqrt{\gamma_L^D}$ of pro*

When the probes that are amphoteric (acidic and basic vapors) are injected into the column, the free energy of desorption (or adsorption) ΔG^{SP}, corresponding to specific interactions, which is given by

$$-\Delta G^{SP} = \mathrm{RT\ Ln}\left(\frac{V_N^{SP}}{V_N^{ref}}\right) \qquad [3\text{-}8]$$

where V_N^{SP} and V_N^{ref} are the retention volumes of polar probes owing to specific interactions and retention volumes of n-alkanes (as the reference line) owing to dispersion forces, respectively.

The determination of ΔG^{SP} for specific probes is demonstrated in Figure 3-2. The vertical difference between the polar probe and alkane line gives the specific energy of interaction ΔG^{SP}.

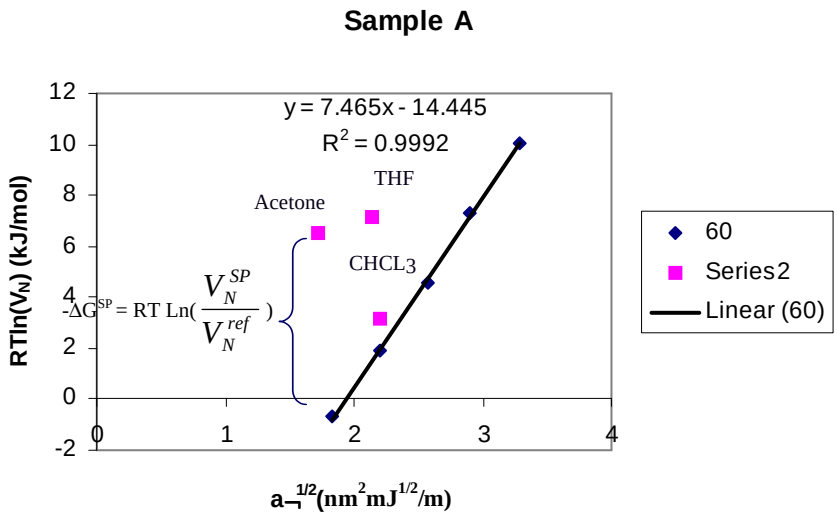

Figure 3-2. *Representation of IGC data used for the determination of ΔG^{sp} for the specific probes.*

In the same way, the calculation of the free enthalpy of desorption or adsorption, ΔH^{SP}, corresponding to specific interaction is given by

$$\Delta G^{SP} = \Delta H^{SP} - T\Delta S^{SP} \qquad [3\text{-}9]$$

ΔH^{SP} and ΔS^{SP} are determined as the slope and intercept of the plot of $-\Delta G^{sp}/T$ versus 1/T respectively (see Figure 3-3).

From the values of ΔH^{sp}, and from the AN and DN values of some specific adsorbates, the acceptor and donor constants, K_A and K_D for the adsorbent can be obtained using the expression (Shultz and Lavielle, 1989):

$$\Delta H^{SP} = K_A \bullet DN + K_D \bullet AN \qquad [3\text{-}10]$$

where DN and AN are the donor and acceptor numbers, respectively, of the acid-base prob. AN and DN numbers for the probes were determined experimentally by NMR (Gutmann, 1978). The quantity of ΔH^{SP}/AN is linearly depended on DN/AN and thus K_A is obtained from the plot as the slope, while K_D is obtained as the intercept.

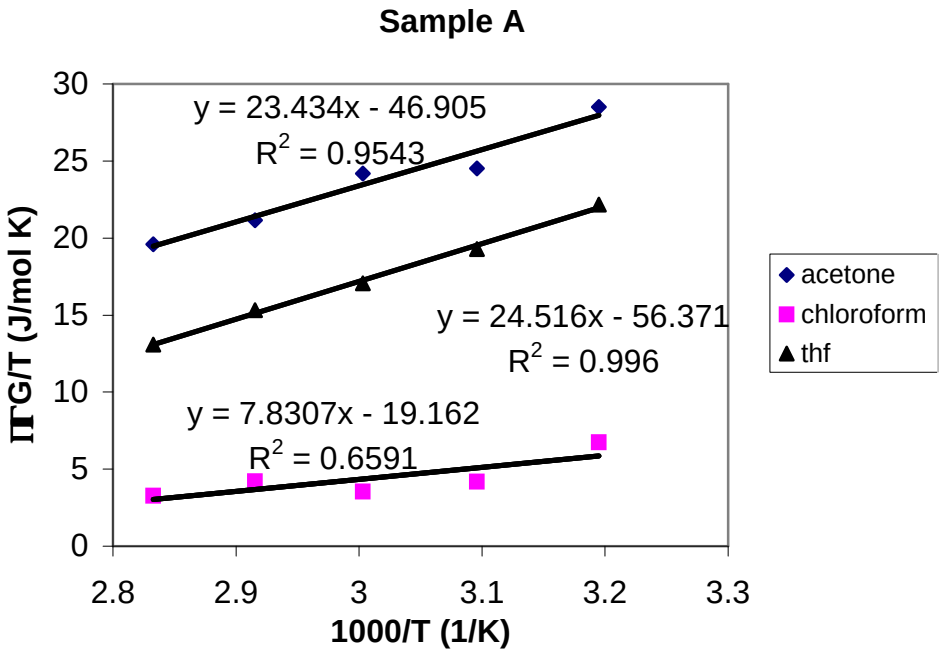

***Figure 3-3**. Representation of IGC data used for the determination of ΔH^{sp} for specific probes.*

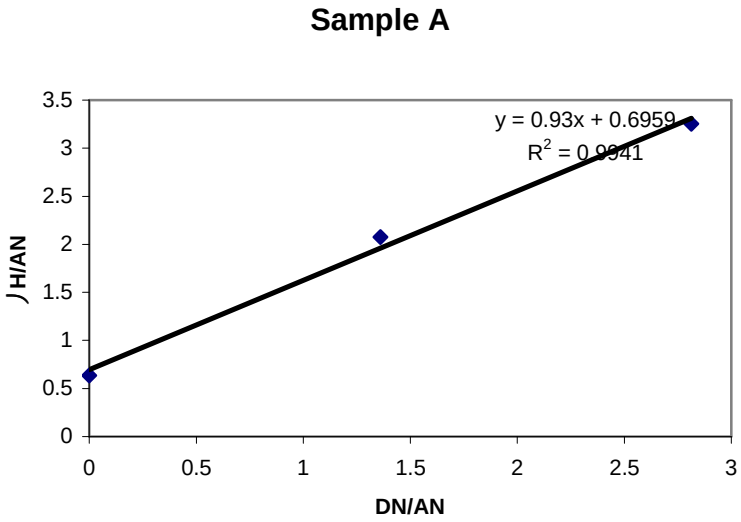

***Figure 3-4.** Plot of $\Delta H^{sp}/AN$ as a function of DN/AN allowing the determination of the acceptor constant K_A and the donor constant K_D.*

3.2 Experimental

3.2.1 Materials

Cellulose fiber: In all experiments, a bleached sulfite pulp obtained from East Texas Pulp and Paper Company is used.

Adsorbates: Adsorbates representing vapors with only dispersion-force interaction capabilities were n-pentane (n-C5), n-hexane (n-C6), n-heptane (n-C7), n-octane (n-C8), and n-nonane (n-C9). Chloroform (CHCl3), acetone, and tetrahydrofuran (THF) represented acidic, basic, and amphoteric vapors capable of interacting specifically. All adsorbates were of analytical grade and were used as received.

Table 3-1. Characteristics of IGC probes used in experiment (Shen and parker, 1999; Coupas et al., 1998).

Probe molecule	A $(Å)^2$	γ_L^D (mJ/ m^2)	AN	DN (kcal/mol)	Specific characteristic
C_5H_{12}	45.55	16.1	0	0	neutral
C_6H_{14}	51.5	18.4	0	0	neutral
C_7H_{16}	57.0	20.3	0	0	neutral
C_8H_{18}	62.8	21.3	0	0	neutral
C_9H_{20}	68.9	22.7	0	0	neutral
Acetone	42.5	16.5	17	12.5	amphoteric
$CHCl_3$	45.0	25.9	23.1	0	acidic
THF	45	19.2	8	20	basic

The characteristics of adsorbates are listed in Table 3-1. The A stands for the molecular surface area of the probes.

3.2.2 Methods

3.2.2.1Fiber treatments:

The following samples were prepared in order to compare the surface properties of fibers before, and after quaternization:

A – sample swelled in water 24 hours

B - mercerized sample for 24 hours

D - the sample B quaternized for 24 hours

All of samples were freeze dried, ground to passe #40 mesh and then dried under vacuum at 45 ^{o}C for 12 hours before packing into a column.

3.2.2.2 Inverse gas chromatography:

A 0.5 m long stainless steel column of 0.635 cm o.d. was used. Between 1.98 g and 2.65 g of freeze-dried and ground cellulose was carefully packed into the column using a handy massager.

Measurements performed on a HP 5790A Gas Chromatograph equipped with a flame ioniztion detector. Helium at 15 ml/min was used as the carrier gas. Methane was used as an inert marker for the dead volume of the column. To assure conditions near zero coverage and no interactions between the injected probes and the cellulose, very small quantities (0.5 µml) of probe vapor were injected. Injections were made from 1 microliter Hamilton syringes, and each injection was repeated several times, showing that the elution peaks were reproducible. The measurements were performed at five different temperatures in the range 40 – 80 ^{o}C.

3.2.2.3 Moisture regains:

The freeze-dried samples were kept in a vacuum oven at 45 ^{o}C for 12 hours and then samples conditioned at 65% RH and 20 ^{o}C for 24 hours. Moisture regain was determined by

$$\text{M.R.} = \frac{W_{wet} - W_{dry}}{W_{dry}} \% \qquad [3\text{-}10]$$

Where W_{dry} and W_{wet} are the weight of samples before and after the samples were put into a conditioned room respectively.

The accessibility of a cellulose sample is derived assuming the maximum moisture regain (MR) for completely accessible cellulose at 65% relative humidity is 17.0% (Jeffries et al., 1968)

$$\% \text{ Accessibility } (A_{H2O} \text{ vap}) = 100MR/17.0 \qquad [3\text{-}11]$$

3.2.2.4 Crystallinity:

X-ray data were obtained in reflection mode by a Rigaku RU-200 BH with Ni-filtered Cu-Kα radiation (λ = 1.54 Å) generated at 40 kV and 40 mA. The scanning was performed through 2θ = 10^{o} to 40^{o} and the scanning speed was 2 degree/min at 0.05 sampling interval. The crystallinity index (CrI) was calculated as

$$\text{CrI} = \frac{I_{002} - I_{am}}{I_{002}} \qquad [3\text{-}12]$$

Where I_{002} is the overall intensity of the peak at 2θ about 22^{o} and I_{am} is the intensity of the baseline at 2θ about 13^{o} and 18^{o} for mercerized and normal cellulose fiber respectively (Segal et al., 1959).

The other way to measure crystallinity is carried out using a Perkin Elmer System 2000 FT-IR. Freeze-dried cellulose powder (1.5 mg) and KBr (200 mg) were homogenized using a vibrator mixture for 30 second and thereafter pressed into an almost transparent

tablet at 167 MPa for 5 minutes. The pellets were analyzed in the absorbance mode with a resolution of 2 cm^{-1} in the range 4000 – 370 cm^{-1}. The total crystallinity index (TCI) is calculated by (Colom and Carrillo, 2002):

$$TCI = \frac{a_{1376}}{a_{2902}} \qquad [3\text{-}13]$$

Where a_{1376} and a_{2902} are the adsorption bands at 1376 and 2902 cm^{-1} respectively.

3.2.2.5 Analysis of Chemical Constitution:

The results were obtained by Perkin Elmer System 2000 FT-IR. The spectra were compared before and after quaternization. The sample preparation and test conditions were the same as mentioned above.

3.2.2.6 Scanning Electron Microscopy (SEM):

A Zeiss DSM 940 SEM made in Germany was used for observation of surface characteristics. The images of each sample were obtained at 500 and 2000 magnification. The samples of each freeze-dried cellulose fiber were mounted onto double-sided adhesive tape over aluminum stubs and sputtered with gold under vacuum prior to the observation.

3.3 Results and Discussion

The dispersive interactions between non-polar probes and tested polymers are discussed first. The net retention times of n-alkanes at different temperature fit an exponential curve (see Figure 3-5, Figure 3-6 and Figure 3-7).

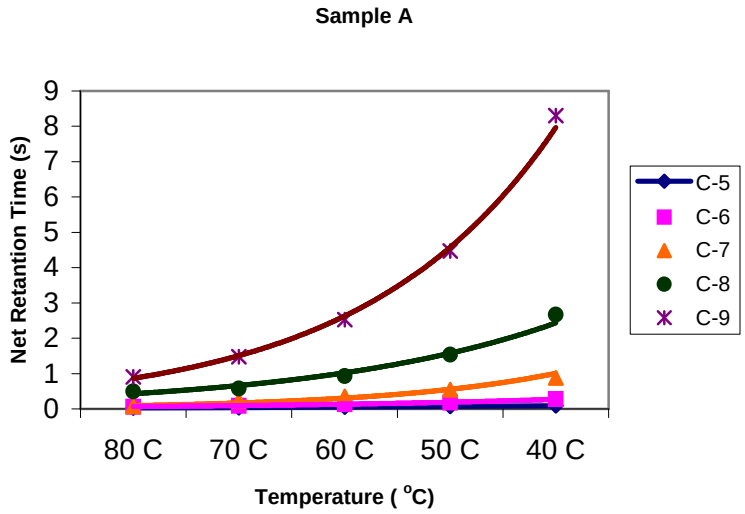

Figure 3-5*. The net retention time of n-alkanes at different temperature for Sample A (control sample).*

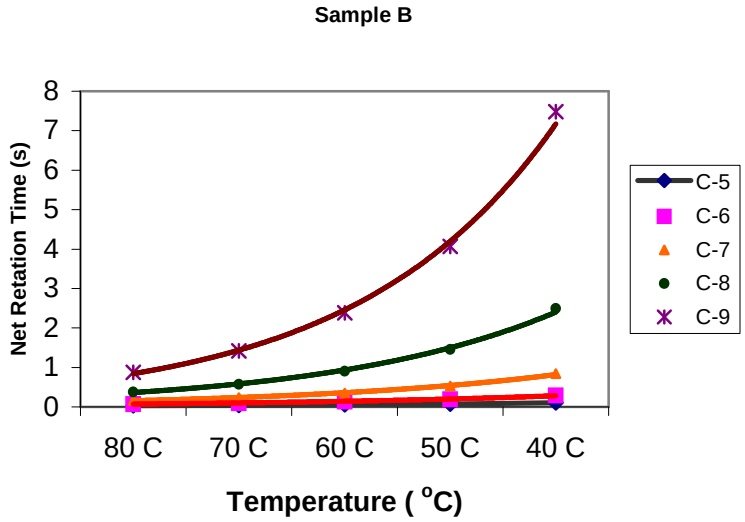

Figure 3-6. *The net retention time of n-alkanes at different temperature for Sample B (mercerized sample).*

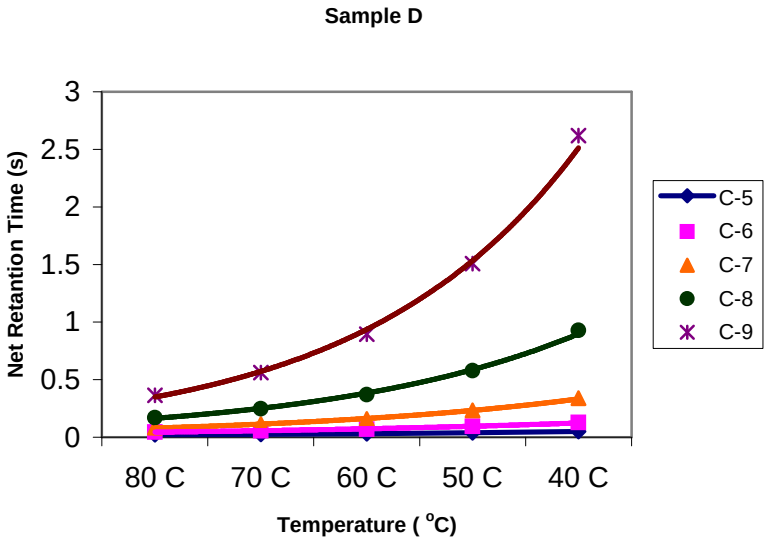

Figure 3-7. *The net retention time of n-alkanes at different temperature for Sample D (quaternized sample).*

The net retention time may reflect the interaction such as London force or dispersive force between n-alkanes and tested polymer powders. It seems that materials with a smaller surface area of a probe are less sensitive to temperature changes; on the contrary, samples with higher surface area of a probe are more sensitive to temperature. For examples, the net retention times of n-pentane for sample A, sample B, and sample D are recorded over the temperature from 40 – 80 ^{o}C. The net retention times of n- nonane was A > B > D over the temperature from 40 – 80 ^{o}C:. From the data of the net retention time, we can establish the relationship between the surface energy of tested polymer powder and the surface energy of probes using equation [3-7] and equation [3-8]. Furthermore, the dispersive components of surface energy can be obtained by the slope of the plot shown in Figure 3-1. The dispersive components of surface energy (γ_S^D) of samples A, B, and D obey a liner relationship over 40 – 80 ^{o}C and also follow the order: A > B > D (see Figure3-8).

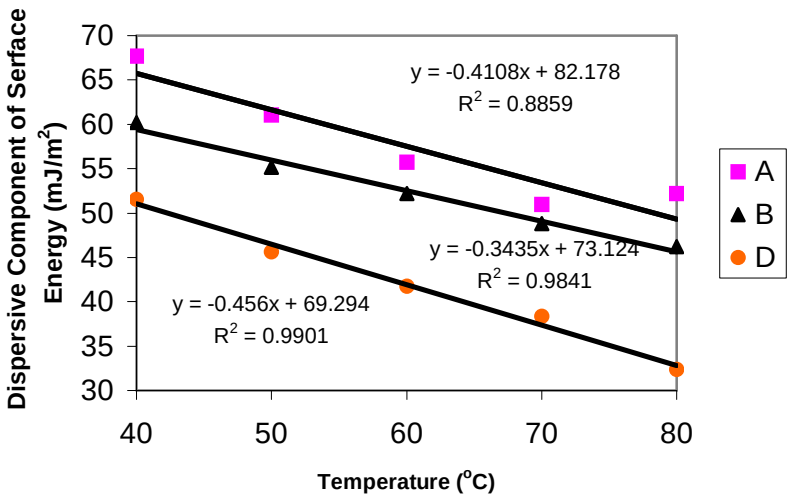

Figure 3-8. *The values of* γ_S^D *versus the temperature.*

The non-polar probes interact with a surface or an interface of polymers through intermolecular forces: a dispersion force, and induced dipole-dipole force. Sample A and B interact with non-polar probes through the dispersion force. Sample D interact with the probes through two forces because the quaternization introduces an ammonium salt that brings positive charges onto polymer chains. Those interactions can be very strong depending on the topological properties of the fibers. The topological properties include the surface areas of fiber and the surface areas of amorphous regions in the fiber.

The explanation of the phenomenon mentioned above can attribute to the supermolecular structure of cellulose fiber. The cellulose fibers consist of elementary fibrils, containing a succession of crystallites and intermediate less-ordered amorphous regions. The crystallites (A) are characterized by their size and their orientation. Less-ordered amorphous regions (B) connect successive crystallites length-wise; they are characterized by their size, density, and orientation. Regions containing laterally bonded molecules (C) connect to laterally adjacent amorphous regions. Cluster formations (D) are

regions where crystallites are fused to large aggregates and region (E) represents the voids (Figure 3-9) (Stana-Kleinschek et al., 2001). The amorphous regions and inner surface area of voids are decisive factors with regard to accessibility, reactivity and adsorption properties of fibers.

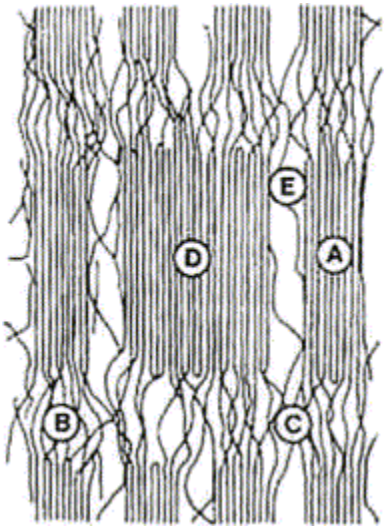

Figure 3-9. *Fine structure of cellulose fibers—schematically: A, crystallites; B, amorphous regions; C, interfibrillar tie molecules; D, cluster formation; E, void (Stana-Kleinschek et al., 2001).*

Thus it is extremely important to explore the supermolecular structures of cellulose fibers before and after quaternization. The crystallinity as determined by X-ray and FT-IR is listed in Table 3-2.

Table 3-2. The X-ray crystallinity index (CrI), FT-IR total crystallinity index (TCI), moisture regain (MR), and accessibility of the samples

Sample	X-Ray CrI	TCI	Moisture Regain (%)	Accessibility (%)
A	0.43	0.73	8.58	50.49
B	0.59	0.78	6.99	41.10
D	0.72	0.84	10.61	62.40

Also the index of the accessibility of cellulose hydroxyl groups calculated from the moisture regain method may be used to estimate the changes of crystallinity. X-ray studies have shown that water molecules do not penetrate the crystalline region (Wadsworth and Cuculo, 1978). Thus the moisture must be absorbed in the amorphous regions and on the surfaces of crystallites. Moisture absorption increases with increasing disorder of the cellulose structure (Saafan et al., 1984). Therefore the accessible areas and crystallinity can well reflect the proportion of two regions. The MR of samples A and B agree with the CrI and CTI. However, in spite of the highest degree of crystallinity, sample D has the highest MR and accessibility.

The supermolecular structures of samples A, B, and D are much different from each other (see Figure 3-14). The crystal structure of sample A corresponds to that of cellulose I. After mercerization and quaternization, the crystal structures become a mixture of cellulose I and cellulose II and the intensity of the peaks increases. That means the crystallinity of cellulose increased after the quaternization. Especially the intensity peak of sample D becomes much shaper than that of sample B. A new peak occurred at $2\theta = 31.9^{o}$. Additionally, the total crystallinity index obtained from FT-IR and the moisture regain data support the results of X-ray. The FT-IR spectra (Figure 3-10) indicate that sample A and sample B display identical fingerprint regions while sample D exhibits a new adsorption peak at 1478.70 cm^{-1} corresponding to $–CH_2-$ stretching, and an asymmetric peak at 895.72 cm^{-1} corresponding to an N^{+}-C stretching vibration that provides evidence for the success of the employed quaternization reaction method (Hashem and El-Shishtawy, 2001).

The topological observations made in SEM experiments also supply additional information. The appearance of sample A shows more hairs and flat cellulose fibers (Figure

3-11) compared with sample B that the appearance becomes round and has more groves on the surface of the fibers (Figure 3-12).

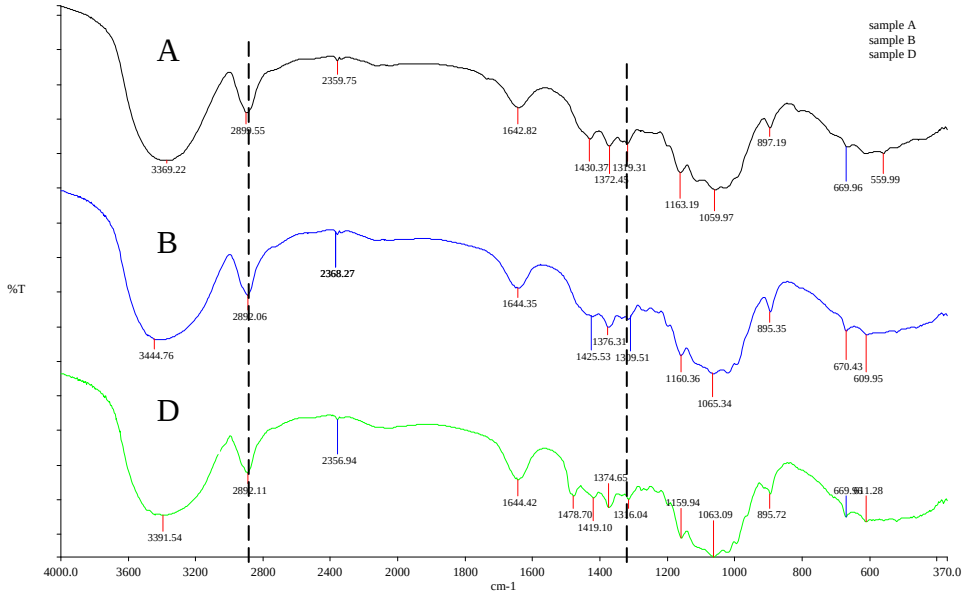

Figure 3-10*. FT-IR spectra for sample A, sample B, and sample D.*

As Table 1-1 indicates that wood pulp contains 40-47% cellulose and 25-35% hemicellulose (Hon, 1996), the hemicellulose can be dissolved in concentrated alkaline solution during the mercerization. The groves that are the evidence of recrystalization and the loss of hemicellulose during mercerization result in increased crystallinity. After quaternization, more deep groves and holes are observed (Figure 3-13). Because quaternization happened at the C-6 position of a cellulose-repeating unit, the quaternary group attached at this position breaks up the intermolecular hydrogen bonding swells cellulose or partially dissolves the cellulose within the amorphous areas in the aquatic solution. The increasing crystallinity of sample D results from the new crystalline formed. The X-ray diffraction signal provides the evidence of new crystals formed at $2\theta = 31.9^{o}$. The partially dissolved cellulose precipitated from the solution and the new crystals were

formed after the quaternized cellulose was washed with distilled water and dried. Cellulose dissolved in solution mixtures of urea and lithium chloride also exhibits same peak at 2θ = 31.9^{o} (Figure 3-14). This is the evidence that recrystallization of quaterinzed cellulose occurs due to the dissolution or partial dissolution after precipitation.

The X-ray, FT-IR, and moisture regain data agree with the results of γ_S^D from Figure 3- 8 for sample A and B. On the other hand, the X-ray and FT-IR data fit the results of γ_D^S, but the moisture regain does not fit due to the change of chemical constituents after quaternization shown above in Figure 3-10. Therefore, the properties of surface and the adsorption behaviors have been totally changed. This change will be discussed below.

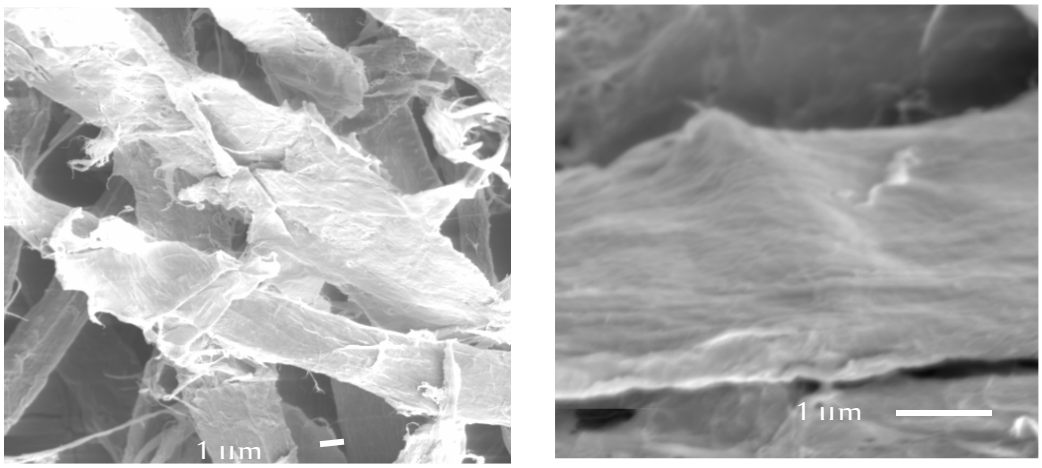

Figure 3-11. *Topological observation of sample A. (a) ×500, (b) ×2000.*

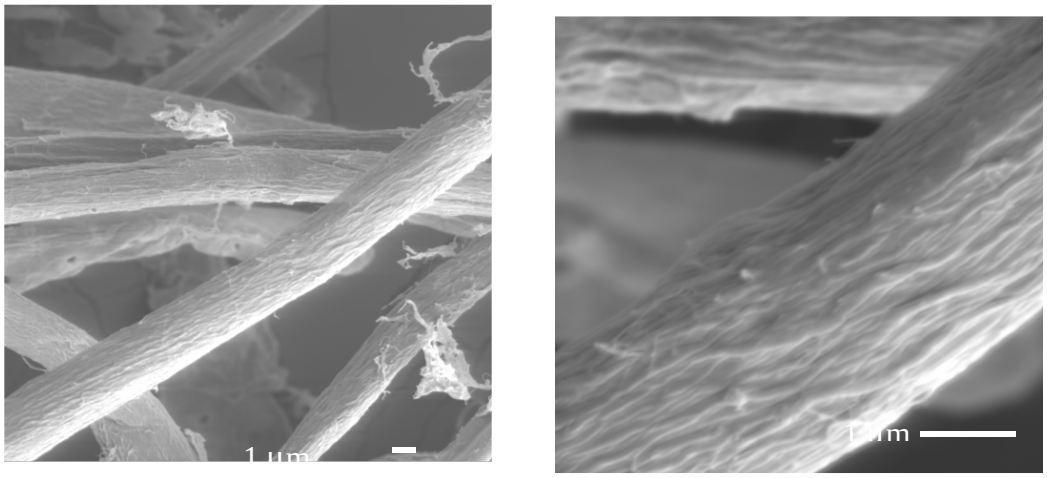

Figure 3-12. *Topological observation of sample B. (a) ×500, (b) ×2000.*

The enthalpy and the entropy of adsorption of the specific probes or polar probes were calculated from the slope and intercept of $-\Delta G^{sp}/T$ versus 1/T, respectively, according to Equation [3-5] and Figure 3-3. The results of enthalpy and entropy of adsorption for sample A, sample B and sample D are listed in Table 3-3.

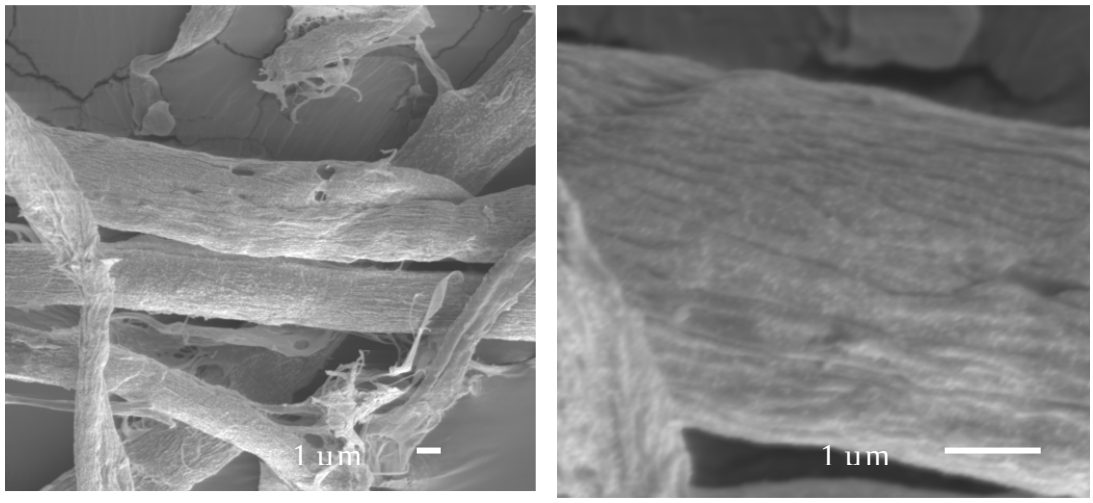

Figure 3-13. *Topological observation of sample D. (a) ×500, (b) ×2000.*

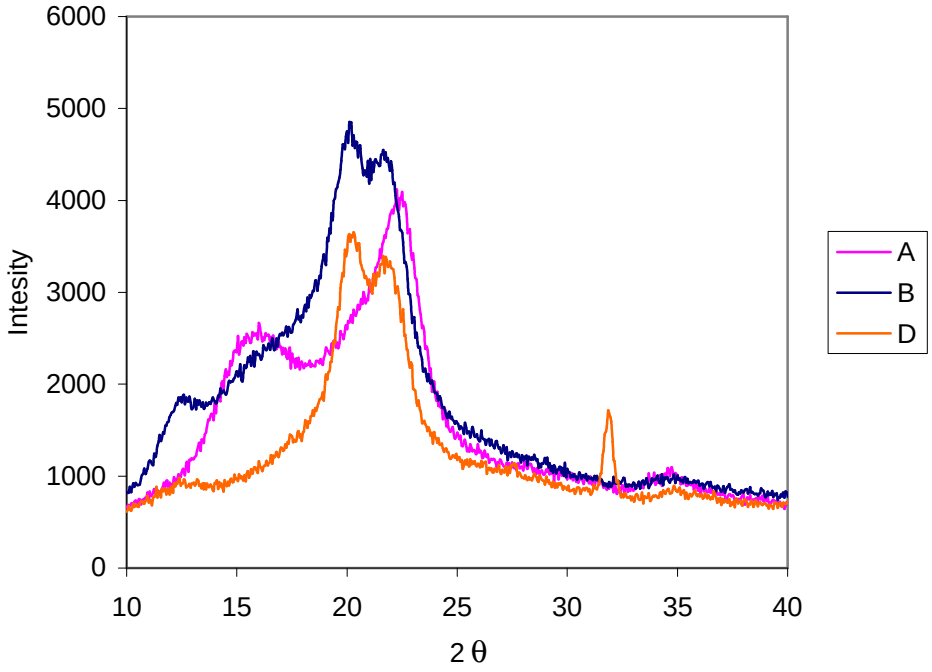

Figure 3-14. *X-ray diffraction curves.*

In the view of thermodynamics, the greater the value of enthalpy, the greater is the reaction or interaction intensity (Santos et al., 2001). Bearing in mind that chloroform ($CHCl_3$), acetone, and tetrahydrofuran (THF) represented acidic, basic, and amphoteric vapors, these compounds are capable of interacting specifically: $-\Delta Hs_P$ of THF is greater than that of $CHCl_3$ before quaternization for sample A and B while $-\Delta H$ of THF is less than that of $CHCl_3$ after quaternization for sample D.

From the values of ΔH^{sp} and from the AN and DN values of the specific adsorbates, the acceptor and donor constants, K_A and K_D for the adsorbents can be obtained using equation [3-6] and Figure 3-4. The K_A and K_D constants of sample A, B and D are shown in the Table 3-4. The K_A constants are greater than the K_D constants of samples A and B. On the contrary, the K_D constants are greater than the K_A constants of sample D.

Table 3-3. The enthalpy and the entropy of adsorption of the specific probes

Sample	-ΔH (J/mol)			ΔS (J/mol*K)		
	Chloroform	Acetone	THF	Chloroform	Acetone	THF
A	14.69	25.96	26.04	-39.20	-54.28	-60.83
B	3.99	24.45	19.5	-7.93	-50.89	-42.77
D	34.45	47.72	30.74	-105.31	-55.28	-94.09

Compared K_A and K_D before and after quaternization, the surface nature of cellulose become more basic than acidic after quaternization. The attached quaternary ammonium salt on the polymer back bone plays a critical role on the properties of surface adsorption.

Table 3-4. Comparison of K_A and K_D

Sample	K_A	K_D
A	0.93	0.66
B	0.8	0.41
D	0.97	1.23

3.4 Conclusions

1. The net retention time of neutral probes with large molecular size is more sensitive to temperature while that of neutral probes with smaller molecular size is less sensitive to temperature. The net retention time is correlated to the fraction of amorphous areas present in the cellulose materials.

2. The dispersive components of surface energy derived from the net retention time increase with increasing the amorphous areas. That is because the non-polar probes can penetrate the amorphous areas of fibers.

3. The surface characteristics of cellulose become more basic than acidic after quaternization in terms of K_A and K_D. Therefore the driving force of adsorption is the heat of Lewis acid-base interaction.

3.5 References

Belgacem, M. N.; Blayo, A.; Gandini, A. *J. Colloid Interface Sci.* **1996**,*182*, 431-436.

Colom, X.; Carrillo, F. *European Polym. J.* **2002**, *38*, 2225- 2230.

Coupas, A. C.; Gauthier, H.; Gauthier, R. *Polym. Composites* **1998**, *19*(3), 280-286.

Dorris, G. M.; Gray, D. G. *J. Colloid Interface Sci.* **1980**, *77*, 35.

Felix, J. M.; Gatenholm, P. *Nordic Pulp Paper Res. J.* **1993**, *1*, 200-203.

Fowkes, F. M. *J. Adhesion Sci. Technol.* **1987**,*1*, 7 – 27.

Gurnagul, N.; Gray, D. G. *J. Pulp Paper Sci.* **1985,** *11*(4), 98-101.

Gutmann, V. *The donor-acceptor approach to molecular interaction*; Plenum: New York, 1978; p 204.

Hashem, A.; El-Shishtawy, R. *Adsorption Sci. Technol.* **2001**, *19*(3), 197- 210.

Hegedus, C. R.; I. L. Kamel. *J. Coatings Technol.* **1993**, *65*, 23-29.

Hon, DN-S. in *Chemical modification of lignocellulosic materials*. Hon DN-S, Ed.; Marcel Dekker: New York, Basel, Hong Kong, 1996; p114.

Jeffries, R.; Roberts, J. G.; Robinson, R. M. *Text. Res. J.* **1968**, *38*, 234-224.

Laszlo, J. A.; Dintzis, F. R. *J. Appl. Polym. Sci.* **1994**, *52*, 531-538.
Laszlo, J. A. *Am. Dyest. Rep.* **1994**, *83*(3), 17-21.

Laszlo, J. A. *Text. Chem. Colori.* **1996**, *28*(5), 13-17.

McClain, M. A.; Wang, W. J.; Hall, D. *Journal of Environmental Monitoring and Restoration*, proceeding, Georgia, 2003.

Mukhopadhyay, P.; Schreiber, H. P. *Colloid Surf. A: Physicochem. Eng. Aspects* **1995**, *100*, 47.

Papirer, E.; Brendle, E.; Balard, H.; Vergelati, C. *J. Adhes. Sci. Technol.* **2000**, *14*(3), 321-337.

Reidl, B.; Kamdem, P. D. J. *Adhes. Sci. Technol.* 1992, 6, 1053.

Reutenauer, S.; Thielmann, F. *J. Mat. Sci.* **2003**, *38*, 2205-2208.

Saafan, A. A.; Kandil, S. H.; Habib, A. M. *Text. Res. Insti.* **1984**, 863 – 867.

Santos, J. M. R. C. A.; Gil, M. H.; Portugal, A.; Guthrie, J. T. *Cellulose* **2001**, *8*, 217-224.

Schultz, J. and Lavielle, J. in *Inverse Gas Chromatography;* Lioyd, D. R.; Ward, T. C.; Schreiber, H. P. Eds; ACS Symposium Series, 391. Am. Chem. Soc., Washington DC, 1989; pp. 185.

Shi, W.; Xu, X.; Sun, G. *J. Appl. Polym. Sci.* **1999**, *71*, 1841-1850.

Schultz, J. L.; Lavielle; C. Martin. *J. Adhes.* **1987**, *23*, 45 – 60.

Shen, W.; Parker, I. H. *Cellulose* **1999**, *6*, 41-55.

Simkovic, I.; Mlynar; J.; Alfoldi, J. *Carbohydr. Polym.* **1992**, *17*, 285-288.

Simkovic, I.; Laszlo, J. A. *J. Appl. Polym. Sci.* **1997**, *64*, 2561-2566.

Stana-Kleinschek, K.; Kreze, T.; Ribitsch, V.; Strnad, S. *Colloid Surf. A: Physicochem. Eng. Aspects* **2001,** *195*(1-3), 275-284.

Tshabalala, M. A. *J. Appl. Polym. Sci.* **1997**, *65*, 1013-1020.

Tze, W. T., Gardner D. J. *J. Adhes. Sci. Technol.* **2001**, *15*(2), 223-341.

Voelkel, A. *Chemometrics and Intelligent Lab. Syst.* **2004**, *72*, 205-207.

Wadsworth, L. C.; Cuculo, J. A. *In Modified Cellulose*, Rowell Ed.; Academic Press, Inc.: New York, 1978; pp117-146.

CHAPTER 4

STUDY ON THE CORRELATION BETWEEN THE SURFACE CHARACTERISTICS AND ADSORPTION CAPABILITY OF QUATERNIZED CELLULOSE FIBER

4.1 Introduction

Very high dye adsorption capability of quaternized cellulose has been demonstrated in Chapter 2. Much less is known about the correlation between the surface characteristics and the adsorption capabilities of quaternizaed cellulose fiber. Therefore, it is very important to understand the driving force for the interactions between the dye molecule and the polymer adsorbent.

According to modern chemistry, a Lewis base is any substance that has electron density that can be shared with another substance in a chemical reaction, and a Lewis acid is any substance capable of accepting electron density from a Lewis base. The Lewis acid-base concept and its more modern generalizations give a comprehensive description of a large class of interactions between organic molecules. This concept has been successfully applied to predict solubility, solvent effects on chemical reactions and many other solvation phenomena. The acid-base concept was also introduced in the theory of adhesion. The results showed that basic polymers interact strongly with acidic surfaces and vice-versa, giving rise to high adhesion strength.

Fowkes (1987) discussed the role of acid-base interactions in term of contact force. All polymers except saturated hydrocarbons have acidic or basic sites according to the modern Lewis acid-base theory. Electrons of oxygen, nitrogen, sulfur and similar elements, as well as π-electrons of polystyrene and other polymers containing aromatic groups are basic sites (electron donors, following the Lewis theory). On the other hand, halogenated hydrocarbons, nitro groups and, in general, all electrophilic sites are electron acceptor; and thus are Lewis acids. The acid-base interaction between polymers and their surroundings (other polymers, solvents, plastizer, filler, etc.) control the strength of the contact interaction, whose enthalpy can be described by the four-constant Drago's equation (Drago, 1994; Mukhopadhyay and Schreiber, 1995):

$$-\Delta H^{ab} = C_a C_b + E_a E_b \qquad [4\text{-}1]$$

where the E terms relate to the electrostatic contributions, the C terms involve covalent contributions to the overall acid-base interactions, and the subscripts a and b denote acid and base. The two constants for the base (subscript b) and two (subscript a) for the acid emphasize that the strength of the acid-base interaction depends not only the ability to donate or accept electrons but also on the polarizability. As Fowkes points out, hydrogen bonding can be considered a subset of acid-base interactions, since its enthalpy can be accurately described by the Drago equation [4-1]. Energy contributions that vary with the strength of the donor-acceptor interaction will be incorporated into the E and/or C parameters obtained from fitting the experimental data (Drago, 1994).

In this chapter, the interactions between the surfaces of the quaternized cellulose fibers and dyes are predicted by acid-base parameters obtained from inverse gas chromatography (IGC). A correlation between the acid-basic characteristics and adsorption capability of quaternized cellulose fiber has been established by IGC.

4.2 Experimental

4.2.1 Materials

Samples A, B and D are described in Chapter 3 and the bleached wood pulp for beating experiments was supplied by the Chemical Engineering Department of Auburn University. The adsorbates for IGC are the same as used in Chapter 3.

The dye for adsorption experiments, Acid Blue (C.I. 42755; FW 737.71), was purchased from Acros Organics and was dried in a vacuum oven at 45 ^{o}C for 24 hours. Then the dried dye was stored in a desiccator.

4.2.2 Methods

4.2.2.1 Fiber Treatments

The bleached wood pulp was blended for 5 minutes in a certain amount of distilled water. The blended wood pulp was used as an unbeaten fiber (sample 0). Then the blended wood pulp was beaten using VOITH Beater at 10 and 50 minutes (samples 10 and 50).

4.2.2.2 Measurements of Freeness

The freeness of pulp is designed to give a measure of the rate at which a dilute suspension of pulp (3g of pulp in 1 L of water) may be drained (according to TAPPI T227 om-92). Since the measurement was carried out in solution at 30 ^{o}C, we have to correct the number to 20 ^{o}C using the chart of freeness corrections.

4.2.2.3 Quaternization of Beaten Fibers

In order to study the surface increase after beating, samples 0 and 50 were reacted with quaternary ammonium under the same conditions (Method A mentioned in Chapter 2) for 1 hour, resulting in samples 0-N and 50-N respectively. Another sample, 50-N-30H, was reacted with quaternary ammonium for 30 hours under the same reaction conditions previously used.

4.2.2.4 Nitrogen Analysis

The samples were freeze dried for 24 hours and then dried at 45^{o}C under vacuum in a vacuum oven for another 12 hours. The nitrogen contents were determined using a LECO CN-2000 instrument at 1050^{o}C. The analysis was performed at the Soil Test Lab of Auburn University.

4.2.2.5 Analysis of Chemical Constitution

The data were obtained from Perkin Elmer System 2000 FT-IR and spectra were compared before and after quaternization. Sample preparation and test conditions were the same as mentioned in Chapter 2.

4.2.2.6 Scanning Electron Microscopy (SEM)

Sample preparation and instrumentation are the same as described in Chapter 2.

4.2.2.7 Kinetic Dye Adsorption

Quaternized cellulose fibers (400 mg dried fiber) were placed into 200 mL of dye solution containing 1.6 g/L of Acid Blue 22 (C.I. 42755) at room temperature with vigorous stirring. The concentrations of the dye in the solution at specific time intervals (1 min, 5 min, 30 min, 1 hour, 8 hours, and up to 24 hours) were detected using a GeneSys 6 spectrophotometer (λ_{max} = 559 nm). Then the saturation value, [S] was determined when the curve is leveling off as the $[D]_s$ (mol/kg) versus time (hour) curve is plotted.

4.2.2.8 Adsorption isotherm

For the adsorption experiments, precisely weighed quaternized cellulose was placed in 50 ml of solutions containing various dye concentrations. The equilibrium isotherm was determined from experiments using ten flasks containing the same amount of adsorbent, mixed with different concentration of dye. The liquor ratio is approximately 1:300, and the dye concentrations varied from 50 mg/L to 2.5 g/L of dye.

Each of the flasks containing quaternized cellulose fibers and the dye solution were placed in a constant temperature water bath and agitated at 25^{o}C. After 24 hrs, the solution samples were filtered using a glass filter. The filtrate of each solution was taken out to measure the residual concentration of the dye solution. Concentrations of the dye in the solutions ($[D]_s$) was measured using a GeneSys 6 spectrophotometer (λ_{max} = 559 nm) to determine the amount of dye on the cellulose fibers ($[D]_f$). Then the saturation value, [S] was determined when the curve is leveling off as the $[D]_s$ verse $[D]_f$ curve is plotted.

4.3 Results and Discussion

4.3.1 Fine structure versus base-acid interaction on dye adsorption

In our study, three samples: water swelled cellulose (sample A), mercerized cellulose (sample B), and quaternized cellulose (sample D) were packed into the IGC column to investigate the interaction between the fibers and probes over the temperature range of 40 to 80 ^{o}C. Enthalpies of interaction derived from IGC data are listed in Table 4-1. The enthalpy significantly increased after quaternization due to the electron donor group, electron acceptor, as well as a very strong positive charge introduced into the polymer chains. This phenomenon fits the Drago equation [4-1].

The data generated in this study are derived from the fundamental parameter in IGC measurements, the specific retention volume, by injecting neutral probes such as saturated n-alkanes and by injecting amphoteric, acidic and basic probes such as acetone, chloroform and THF.

A comparison of K_A and K_D before and after quaternization, included in Table 4-2, shows that the surface nature of cellulose becomes more basic than acidic after quaternization in terms of electron acceptor and electron donor constants, or Lewis acidity

and Lewis bacicity constants. The changes of surface properties result from the changes of chemical constituents revealed by FT-IR (see Figure 3-10).

Table 4-1. The enthalpy and the entropy of adsorption of the specific probes

Sample	-ΔH (kJ/mol)			ΔS (J/mol*K)		
	Chloroform	Acetone	THF	Chloroform	Acetone	THF
A	14.69	25.96	26.04	-39.20	-54.28	-60.83
B	3.99	24.45	19.50	-7.926	-50.89	-42.77
D	34.45	47.72	30.74	-105.31	-55.28	-94.09

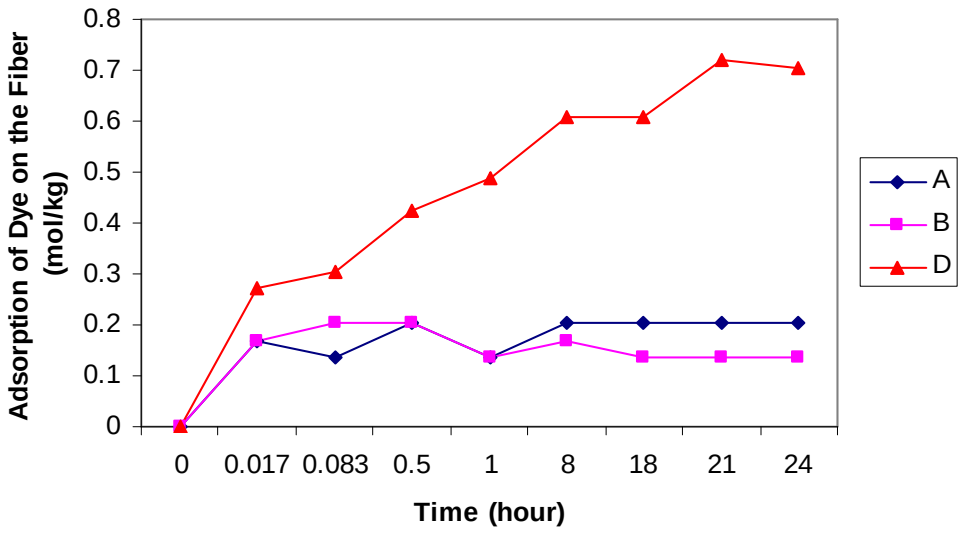

Figure 4-1. *Kinetic dye adsorption.*

Presented in Table 4-3 are data of dye adsorption capability obtained from Figure 4-1. These results show that the saturation value [S] of quaternized cellulose is much higher than that of water swollen and mercerized cellulose. Also Table 4-3 shows that the

surpermolecular structures do not much affect the saturation values since the Samples A and B have different crystallinity indices.

Table 4-2. Comparison of K_A and K_D

Sample	Ka	Kd	R^2
A	0.93	0.66	0.99
B	0.80	0.41	0.89
D	0.96	1.23	0.88

Table 4-3. Comparison of saturation values

Sample	[S] (mol/kg)	N%
A	0.23	0
B	0.14	0
D	0.71	1.5

In all, the high dye adsorption capability of quaternized cellulose mainly depends on the acid-base interaction and the high polarity of the quaternary ammonium salt introduced by the reaction, and the influence of the crystallinity, crystallite size and its orientation on the adsorption character is less important (Kreze et al., 2002).

4.3.2 Surface areas verse base-acid interaction on dye adsorption

The surface area is very important for any kind of adsorptions, no mater which kind of adsorption, either monolayer adsorption (Langmuir model) or multiplayer adsorption. Therefore, beating might be a good way to increase the surface area of the

fibers so as to increase the adsorption capacity. Freeness measures how fast a volume of water can be drained at a specific volume of the mixed solution of water and fibers. The freeness can reflect the surface area and bonding properties (TAPPI, 1992). Table 4-4 shows that the freeness is increased with increasing beating time. Also, the nitrogen content of cellulose after the quaternization under some reaction conditions can reflect the surface areas. On the other hand, the TCI of three samples do not change much. The pictures of SEM can provide a direct way to observe the surface changes before and after beating. The pictures of SEM indicate that cracks and fibrils in wood pulps become more frequent with increasing beating time (see Figure 4-2 and 4-3).

Table 4-4 and the SEM pictures show that the surface area dramatically increased with beating time. However, the IGC data do not show (Figure 4-4) any increase of dispersive components of surface energy, γ_S^D. As mentioned in Chapter 3, γ_S^D is related to the amount of amorphous area. Interestingly the beating does not increase the amount of amorphous area, it is speculated that the crystal is too hard to be broken by the beater and the breaking points are located in the amorphous regions. Therefore, the dispersive components of surface energy do not vary before and after beating because the amorphous regions were not affected by beating.

Table 4-4. The freeness and nitrogen contents of samples

Beaten Time (min)	0	10	50
Freeness (mL)	737	658	38
Nitrogen Contents (%)	0.54	0.66	0.72
TCI*	0.85	0.86	0.88

* Total Crystallinity Index

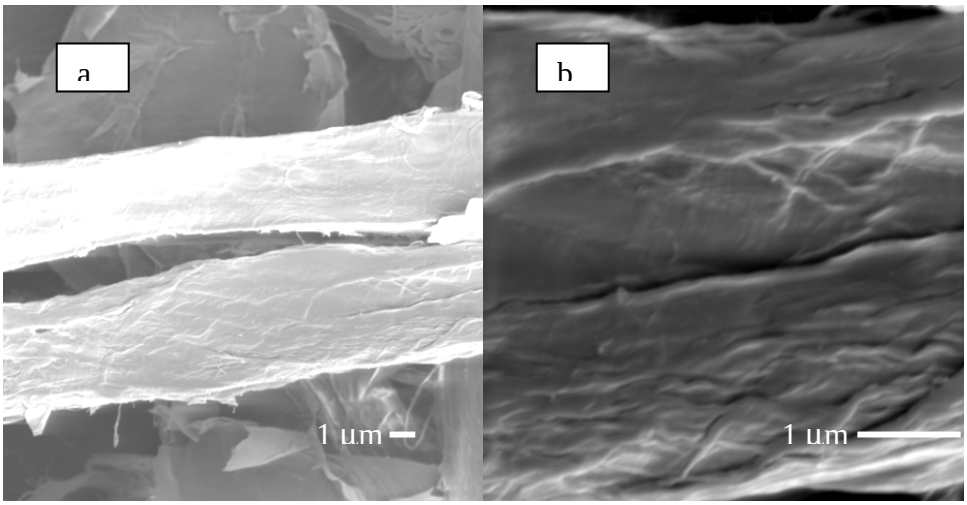

Figure 4-2. *The Morphology of Control Sample (a) ×500, (b) ×2000.*

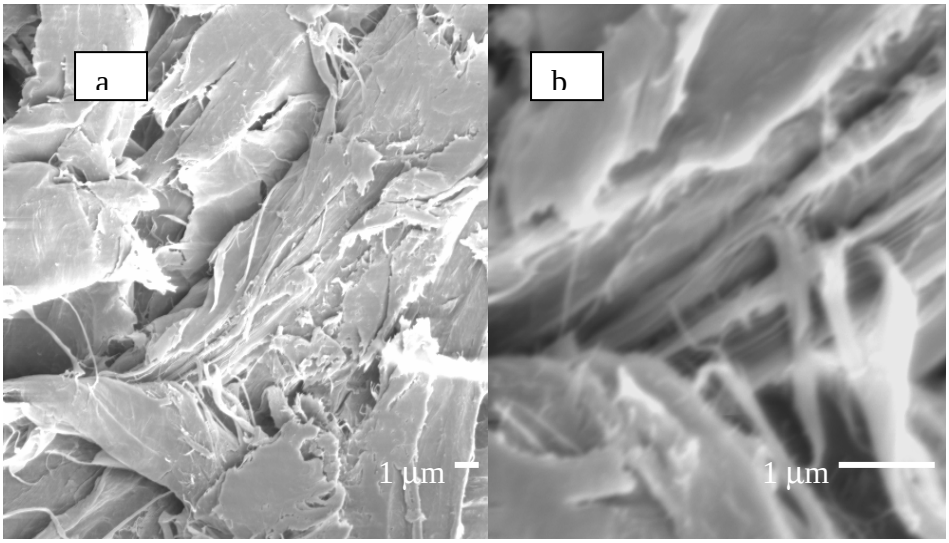

Figure 4-3. *The Morphology of Beaten Sample at 50 Min (a) ×500, (b) ×2000.*

As discussed above, the influence of surpermolecular structures on the adsorption character is less important, and also the mechanical method does not change the crystallinity of beaten fiber, therefore the beaten fiber does not increase the adsorption capacity. Figure 4-5 indicates the dye adsorptions of sample 0 and 50 have exactly same saturation values ($[D_s]$ = 0.11 mol/kg) after 24 hours at equilibrium states. This is because beating does not affect the surface chemical composition (Fardim and Duran, 2003). Also

an FT-IR spectrum does not show any differences between sample 0 and sample 50 (Figure 4- 6).

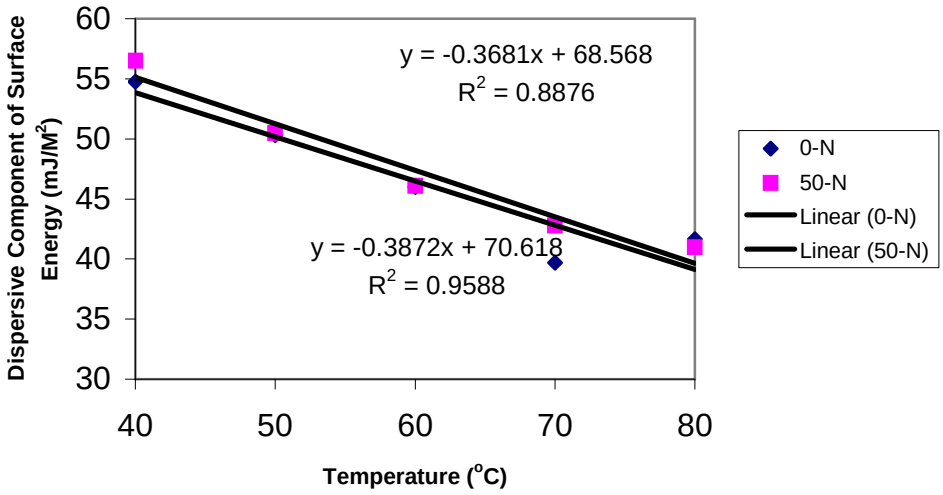

Figure 4-4*. The values of* γ_S^D *versus the temperature.*

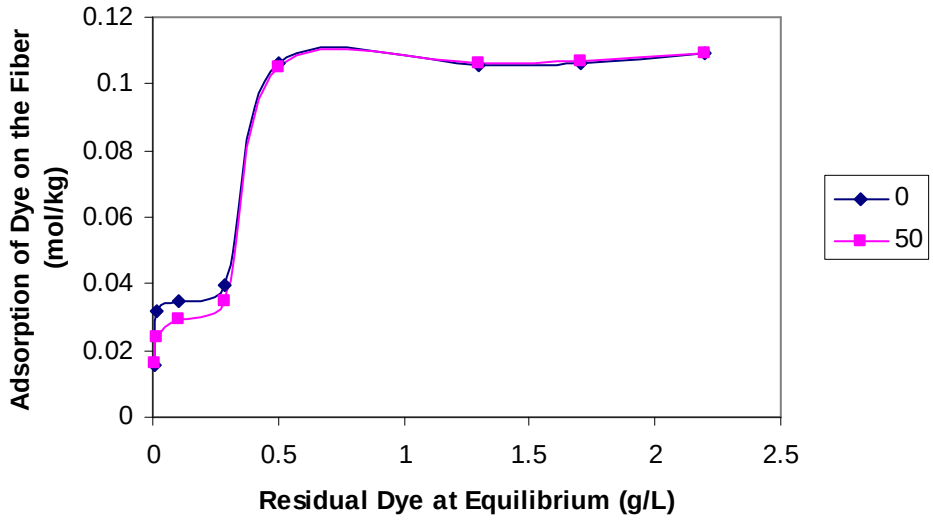

Figure 4-5. *Adsorption isotherm for samples 0 and 50 at 24 hours.*

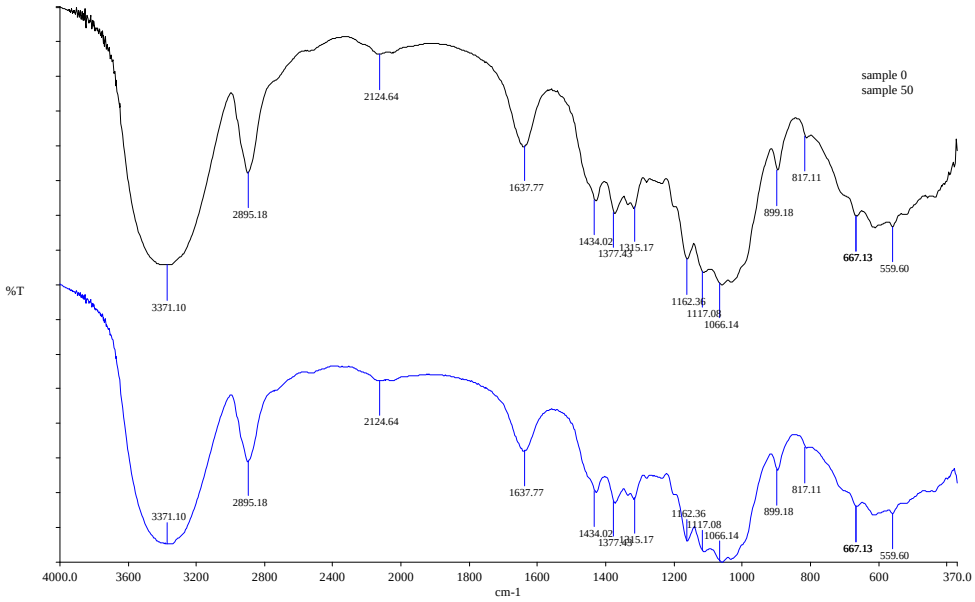

Figure 4-6. *FT-IR spectra for sample 0 and sample 50.*

Compared the dye adsorption capacities after quaternization shown in Figure 4-7 with that of unquaternized cellulose, the saturation values of the quaternized cellulose ($[D_s]$ = 0.57 mol/kg and 0.66 mol/kg) are almost 5-6 times higher those of unquaternized cellulose shown in Figure 4-5. With increasing the reaction time from 1 hour to 30 hours in Figure 4-8, the saturation value of sample 50-N-30H ($[D_s]$ = 1.07 mol/kg) is increased by almost 60% as compared with sample 50-N. The Table 4-5 listed the saturation values compared with nitrogen contents.

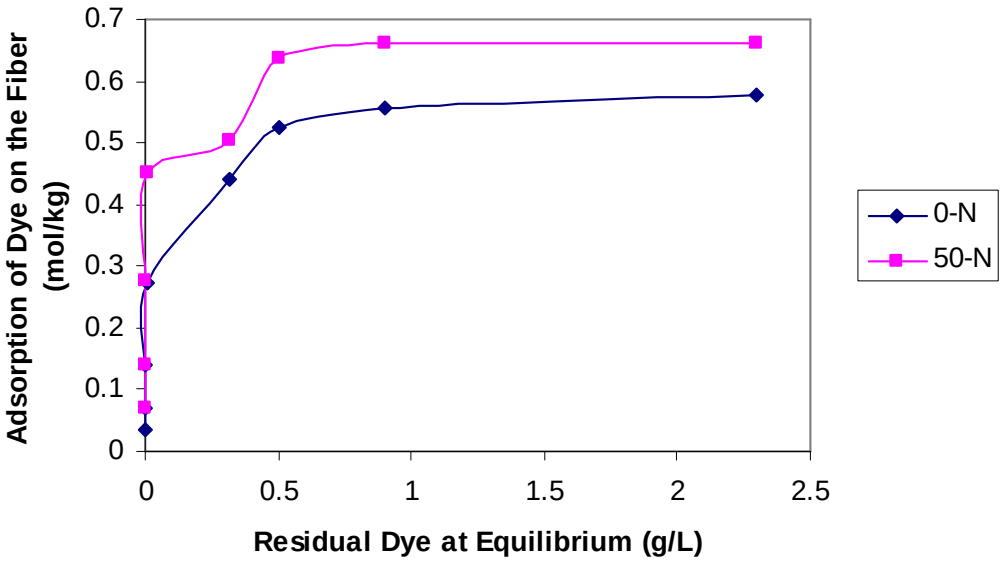

Figure 4-7. *Adsorption isotherm for samples 0-N and 50-N at 24 hours.*

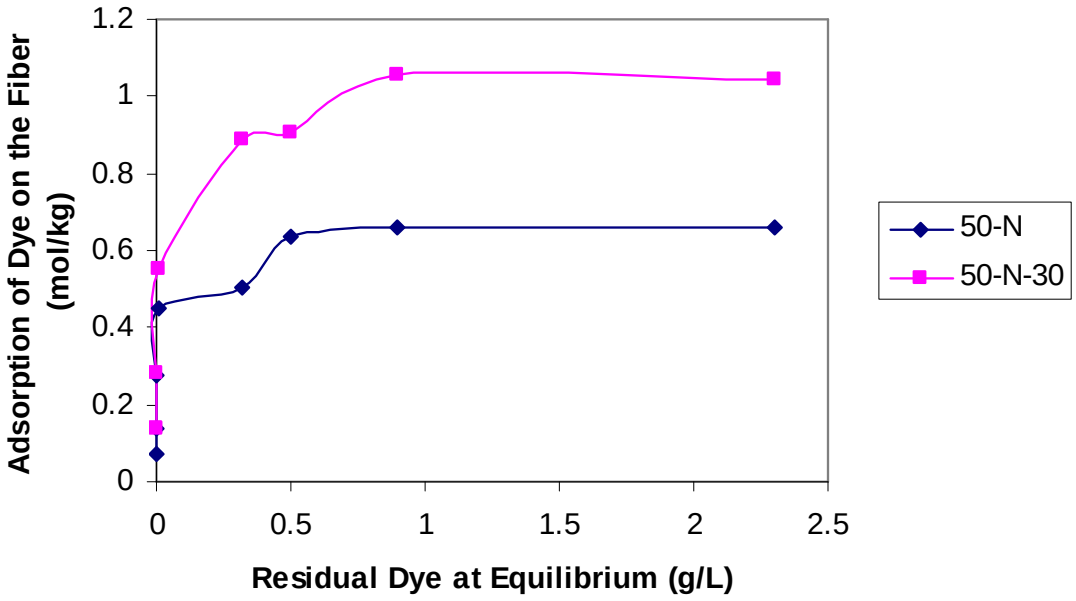

Figure 4-8. *Adsorption Isotherm for samples 50-N and 50-N-30 at 24 hours.*

Table 4-5. The saturation values for different nitrogen contents

Sample No.	[S] (mol/kg)	N%
0	0.11	0
50	0.11	0
0-N	0.57	0.54
50-N	0.66	0.72
50-N-30H	1.07	1.0

The dye affinities of quaternized cellulose fibers increased significantly after quaternization (Giles, 1989). The saturation values and the dye affinities of quaternized cellulose increased because the reaction introduced an electron donor site (-O- group) and a positive charge group (quaternary ammonium). The Figure 4-9 illustrates the interactions between quaternized cellulose and an anionic dye as an example (Rivlin, 1992). The acid-basic interaction takes place between the electron donor (-O-) group and electron acceptor (-N=N-) where a very strong ionic bond is formed between ($-N^+-$) and (SO_3^-). Furthermore, another form of hydrogen bonding is one in which the delocalized electrons of a conjugated ring system provide an electronegative center for involvement in a bond (Rattee and Breuer, 1974). In this case, the benzene groups of dye molecular interact with proton donor or electron acceptor, –OH to form a hydrogen bond.

According to physical chemistry, the higher enthalpy of interaction results in the strong interactions or bonding. The enthalpy between quaternized cellulose fibers and acid/basic probes increases with the nitrogen contents (Table 4-6). The strength of the electrostatic interaction or ionic bonding also increases with nitrogen contents. Thus, the enthalpy of acid-base interaction and ionic bonding (electrostatic interaction) is increased

with increasing nitrogen contents according to the equation [4-1]. Then, the dye adsorption behavior of the quaternized cellulose fibers with different nitrogen contents is able to be predicted by the enthalpy of interactions. The dye affinity and saturation values increase with nitrogen content as shown in Figure 4-7 and Figure 4-8, and the dye affinity and saturation values are summarized in Table 4-7.

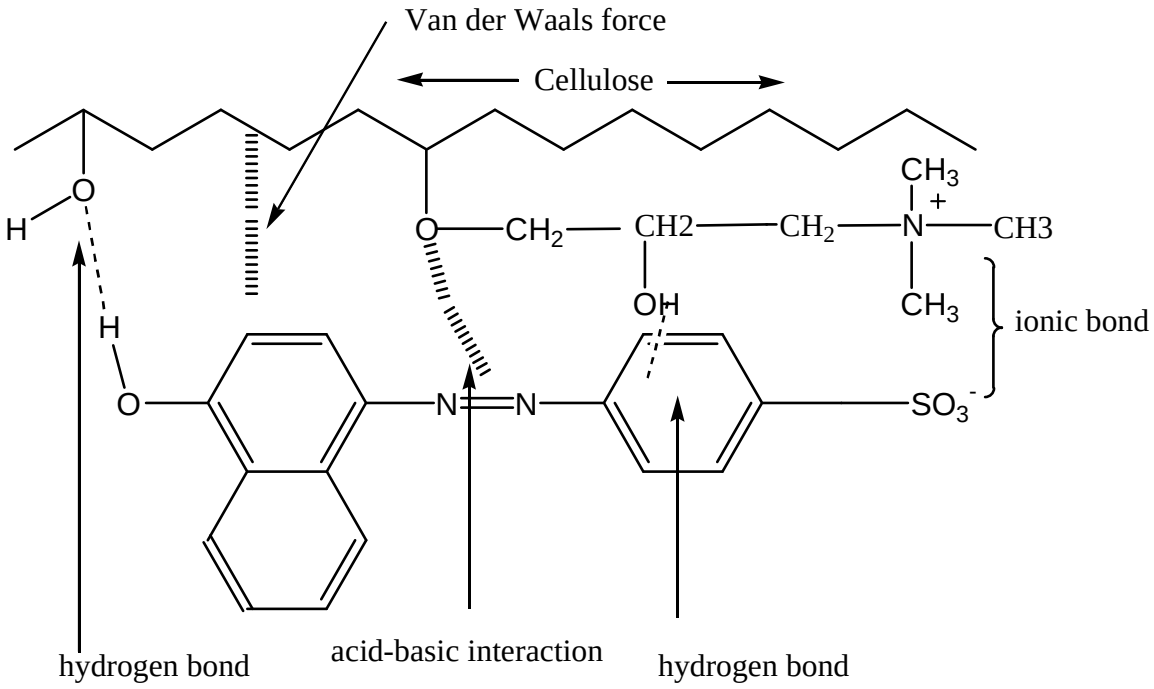

Figure 4-9*. Chemical bonds and interactions between an anionic dye and the quaternized cellulose.*

Table 4-6. The enthalpy and the entropy of adsorption of the specific probes

Sample	-ΔH (kJ/mol)			ΔS (J/mol*K)		
	Chloroform	Acetone	THF	Chloroform	Acetone	THF
0-N	3.0608	15.696	8.528	-4.1543	-29.642	-15.182
50-N	5.0272	13.555	8.7004	-5.0272	-21.669	-14.6

Table 4-7. Comparison of the dye affinity and saturation values of quaternized cellulose with different beating time and reaction time samples

Sample	Affinity (mol/kg)	[S] (mol/kg)	N%
0-N	0.27	0.57	0.54
50-N	0.45	0.66	0.72
50-N-30H	0.54	1.07	1.00

Table 4-8. The proportion of molar numbers of dye and nitrogen

Sample	Dye moles/kg (D)	Quat moles/kg (N)	D/N
0-N	0.57	0.36	1.58
50-N	0.66	0.51	1.29
50-N-30H	1.07	0.71	1.51

The dye adsorption behavior of quaternized beaten wood pulp in acid blue dye is different from the recycled newsprints in Chapter 2 (Figure 4-5, Figure 4-7, and Figure 4-8). The data of Table 4-8 are calculated from Table 4-7 based on 1 kg of quaternized cellulose fibers. Each molecule of quaternary ammonium on the beaten fiber can bond more dye molecules because the D/N is greater than 1. Therefore, the adsorption behavior

does not fit Langmuir isotherm model when the quaternized cellulose reacts with the acid dye.

4.4 Conclusions

The supermolecular structure and surface areas do not affect the capability of adsorption of cellulose because the saturation values of dye adsorption are almost same before and after beating. But the saturation value of dye adsorption is dramatically increased after quaternization because the chemical composition was changed. The increases of the enthalpy of adsorption result from acid-basic interactions and the polarity of cellulose after quaternization.

The chemical constitution plays a critical role for adsorption capabilities. The interactions between dye and quaternized cellulose increase significantly due to the fact that quaternization introduced more acid-base and ion-ion interaction sites. With increasing beating time, the increasing of the surfaces of cellulose fiber results in increasing the reaction probability between cellulose fiber and quaternary ammonium chloride. At the same time, more quaternary ammonium salts are introduced onto the polymer chains with longer reaction time. And the dye adsorption behavior does not fit Langmuir isotherm when the quaternized cellulose react with the acid dye.

4.5 References

Drago, R. S.; Matwiyoff, N. A. *Topics in Modern Chemistry: Acids and Bases*; Raytheon Education Company: Lexington, Massachusetts, 1968.

Drago, R. S. *Applications of Electrosatatic-Covalent Models in Chemistry*; Surfside Scientific Publishers: Florida, 1994; p183.

Fardim, P.; Duran, N. *Colloid and Surf. A: Physicochem. Eng. Aspects,* **2003**, *223*, 263-276.

Finston, H. L.; Rychtman, A. C. A *New View of Current Acid-Base Theories*; John Wiley & Sons: New York, 1982; p70.

Fowkes, F. M. *J. Adhes. Sci. Technol.* **1987**, *1*, 7 – 27.

Freeness of pulp; *Tappi*, T 227 om-92, 1992.

Giles, C. H. in *The theory of coloration of textile*, 2nd ed.; Johnson, A., Ed.; Society of Dyers and Colourists: England, 1989; p 120

Garbassi, F., Morre, M.; Occhiello, E. *Polymer Surfaces From Physics to Technology*. John Wiley & Sons: Chichester, England, 1995; P 332.

Kreze, T.; Jeler S.; Strand, S. *Mat. Res. Innovat.* **2002**, *5*, 227-283.

Larsson, A.; Stenium, P. *Acid-Bade Interactions between Cellulose and Organic Molecules*. International Symposium on Wood Pulping Chemistry. Technical paper; **1985**, p27-28.

Mukhopadhyay, P.; Schreiber, H. P. *Colloids Surf. A: Physicochem. Eng. Apects* **1995**, *100*, 47-71.

Rattee, I. D.; Breuer, M. M. *The physical chemistry of dye adsorption*; Academic Press: London and New York, 1974; p 19.

Rivlin, J. *The Dyeing of Textile Fibers: Theory and Practice*; Pennsylvania, 1992.